

# The exclusive rare decays $B \rightarrow K\bar{l}\bar{l}$ and $B_c \rightarrow D(D^*)\bar{l}\bar{l}$ in a relativistic quark model

Amand Faessler<sup>1</sup>, Th.Gutsche<sup>1</sup>, M.A.Ivanov<sup>2</sup>, J.G.Körner<sup>3</sup>, V.E.Lyubovitskij<sup>1</sup>

<sup>1</sup> Institut für Theoretische Physik, Universität Tübingen,  
Auf der Morgenstelle 14, D-72076 Tübingen, Germany

<sup>2</sup> Bogoliubov Laboratory of Theoretical Physics,  
Joint Institute for Nuclear Research, 141980 Dubna, Russia

<sup>3</sup> Institut für Physik, Johannes Gutenberg-Universität, D-55099 Mainz, Germany

Received:

**Abstract.** We study the exclusive rare decay  $B \rightarrow K\bar{l}\bar{l}$ . We calculate the relevant form factors within a relativistic constituent quark model, for the first time without employing the impulse approximation. The calculated form factors are used to evaluate differential decay rates and polarization observables. We present results on the  $q^2$ -dependence of a set of observables with and without long-distance contributions. A similar analysis is done for the exclusive rare decays  $B_c \rightarrow D(D^*)\bar{l}\bar{l}$  with special emphasis on the cascade decay  $B_c \rightarrow D^*(\rightarrow D\pi)\bar{l}\bar{l}$ . We derive a four-fold angular decay distribution for this process in terms of helicity amplitudes including lepton mass effects. The four-fold angular decay distribution allows to define a number of physical observables which are amenable to measurement. We compare our results with the results of other studies.

PACS: 12.15.Hh, 12.39.Ki, 13.20.He, 14.40.Nd

## 1 Introduction

The flavor-changing neutral current transitions  $B \rightarrow K+X$  and  $B_c \rightarrow D(D^*)+X$  with  $X = \gamma, l^+l^-, \bar{\nu}\nu$  are of special interest because they proceed at the loop level in the Standard Model (SM) involving also the top quark. They may therefore be used for a determination of the Cabibbo-Kobayashi-Maskawa (CKM) matrix elements  $V_{tq}$  ( $q = d, s, b$ ). The available experimental measurements of the branching ratio of the inclusive radiative  $B$ -meson decay

$$\text{Br}(B \rightarrow X_s \gamma) = \begin{cases} (3.11 \pm 0.80(\text{stat}) \pm 0.72(\text{syst})) \times 10^{-4} & \text{ALEPH [1]} \\ (3.36 \pm 0.53(\text{stat}) \pm 0.42(\text{syst})^{+0.50}_{-0.54}(\text{th})) \times 10^{-4} & \text{BELLE [2]} \\ (3.21 \pm 0.43(\text{stat}) \pm 0.27(\text{syst})^{+0.18}_{-0.10}(\text{th})) \times 10^{-4} & \text{CLEO [3]} \end{cases}$$

are consistent with the next-to-leading order prediction of the standard model (see, e.g. [4] and references therein):

$$\text{Br}(B \rightarrow X_s \gamma)_{\text{SM}} = (3.35 \pm 0.30) \times 10^{-4}. \quad (1)$$

The decay  $B \rightarrow K l^+ l^-$  ( $l = e, \mu$ ) has been observed by the BELLE Collaboration [5] with a branching ratio of

$$\text{Br}(B \rightarrow K l^+ l^-) = (0.75_{-0.21}^{+0.25} \pm 0.09) \times 10^{-6}. \quad (2)$$

The recent observation of the bottom-charm  $B_c$  meson by the CDF Collaboration at Tevatron in Fermilab [6] raises hopes that one may also explore the rare decays of the bottom-charm meson in the future.

The theoretical study of the exclusive rare decays proceeds in two steps. First, the effective Hamiltonian for such transitions is derived by calculating the leading and next-to-leading loop diagrams in the SM and by using the operator product expansion and renormalization group techniques. The modern status of this part of the calculation is described in the review [7] (and references therein). Second, one needs to evaluate the matrix elements of the effective Hamiltonian between hadronic states. This part of the calculation is model dependent since it involves nonperturbative QCD. There are many papers on this subject. The decay rates, dilepton invariant mass spectra and the forward-backward asymmetry in the decays  $B \rightarrow K l^+ l^-$  ( $l = e, \mu, \tau$ ) have been investigated in the SM and its supersymmetric extensions by using improved form factors from light-cone QCD sum rules [8]. An updated analysis of these decays has been done in [4] by including explicit  $O(\alpha_s)$  and  $\Lambda_{\text{QCD}}/m_b$  corrections. The invariant dilepton mass spectrum and the Dalitz plot for the decay  $B \rightarrow K l^+ l^-$  have been studied in [9] by using quark model form factors. The  $B \rightarrow K l^+ l^-$  decay form factors were studied via QCD sum rules in [10] and within the lattice-constrained dispersion quark model in [11]. Various aspects of these decays were discussed in numerous papers by Aliev *et al.* [12]. The exclusive semileptonic rare decays  $B \rightarrow K l^+ l^-$  were analyzed in supersymmetric theories in [13]. The angular distribution and CP asymmetries in the decays  $B \rightarrow K \pi e^+ e^-$  were investigated in [14]. The lepton polarization for the inclusive decay  $B \rightarrow X_s l^+ l^-$  was discussed in [15] and [16]. The rare decays of  $B_c \rightarrow D(D^*) l^+ l^-$  were studied in [17] by using the form factors evaluated in the light front and constituent quark models.

In this paper we study the exclusive rare decays  $B \rightarrow K \bar{l} l$ . We employ a relativistic quark model [18, 19] to calculate the decay form factors. This model is based on an effective Lagrangian which describes the coupling of hadrons  $H$  to their constituent quarks. The coupling strength is determined by the compositeness condition  $Z_H = 0$  [20, 21] where  $Z_H$  is the wave function renormalization constant of the hadron  $H$ . One starts with an effective Lagrangian written down in terms of quark and hadron fields. Then, by using Feynman rules, the S-matrix elements describing the hadronic interactions are given in terms of a set of quark diagrams. In particular, the compositeness condition enables one to avoid a double counting of hadronic degrees of freedom. The approach is self-consistent and universally applicable. All calculations of physical observables are straightforward. The model has only a small set of adjustable parameters given by the values of the constituent quark masses and the scale parameters that define the size of the distribution of the constituent quarks inside a given hadron. The values of the fit parameters are within the window of expectations.

The shape of the vertex functions and the quark propagators can in principle be found from an analysis of the Bethe-Salpeter and Dyson-Schwinger equations

as was done e.g. in [22]. In this paper, however, we choose a phenomenological approach where the vertex functions are modelled by a Gaussian form, the size parameter of which is determined by a fit to the leptonic and radiative decays of the lowest lying charm and bottom mesons. For the quark propagators we use the local representation. In the present calculations we do not employ the so-called impulse approximation used previously [19]. The numerical results obtained with and without the impulse approximation are close to each other for light-to-light and heavy-to-heavy transitions but differ considerably from one another for heavy-to-light transitions as e.g. in the  $B \rightarrow \pi$  transitions.

We calculate the form factors of the transition  $B \rightarrow K$  and use them to evaluate differential decay rates and polarization observables. We give the  $q^2$ -dependence of a set of observables with and without long-distance contributions which include the lower-lying charmonium states according to [23]. We extend our analysis to the exclusive rare decay  $B_c \rightarrow D(D^*)\bar{l}l$ . We derive a four-fold angular decay distribution for the cascade  $B_c \rightarrow D^*(\rightarrow D\pi)\bar{l}l$  process in the helicity frame including lepton mass effects following the method outlined in [24]. The four-fold angular decay distribution allows one to define a number of physical observables which are amenable to measurement. We compare our results with the ones of other studies.

We should remark that our approach is developed mainly for the hadrons (mesons and baryons) which satisfy to the so-called "threshold inequality": the hadron mass should be smaller the sum of their constituents, i.e. the sum of the constituent quark masses. In this vein, our model was successfully developed for the study of light hadrons (e.g., pion, kaon, baryon octet,  $\Delta$ -resonance), heavy-light hadrons (e.g.,  $D$ ,  $D_s$ ,  $B$  and  $B_s$ -mesons,  $\Lambda_Q$ ,  $\Sigma_Q$ ,  $\Xi_Q$  and  $\Omega_Q$ -baryons) and double heavy hadrons (e.g.,  $J/\Psi$ ,  $\Upsilon$  and  $B_c$ -mesons,  $\Xi_{QQ}$  and  $\Omega_{QQ}$  baryons) [18, 19]. To extend our approach to other hadrons we had to introduce extra model parameters or do some approximations, like, e.g., to introduce the cutoff parameter for external hadron momenta to guarantee the fulfilment of the mentioned above "threshold inequality". Therefore, at the present stage we can not apply our approach for the study of rare decays involving  $K^*$  mesons. Probably, it will be a subject of our future investigations.

The layout of the paper is as follows. In Sec. II we discuss the effective Hamiltonian. We use the analytical expressions for the Wilson coefficients from [7] and the input parameters from [8]. Sec. III is devoted to the description of the  $B(B_c) \rightarrow K(D, D^*)\bar{l}l$  decays in terms of helicity amplitudes. We derive the four-fold angular decay distribution for the cascade  $B_c \rightarrow D^*(\rightarrow D\pi)\bar{l}l$  process in the helicity system and define a number of physical observables from the angular decay distribution. Our analysis goes beyond the results on the four-fold decay distribution presented in [25, 26] in that we include lepton mass effects appropriated for the treatment of the channel with  $\tau$ -leptons in the final state. We also present results on the longitudinal polarization of the leptons in the  $\bar{l}l$ -CM frame. This analysis differs from the analysis in [25, 26] where the polarization of the leptons were calculated in the initial meson rest system. We also include lepton mass effects in the polarization calculation. In Sec. IV we briefly discuss our relativistic quark model and demonstrate the difference between the exact calculation and the approximate calculation using the impulse approximation

taking as an example the  $B - \pi$  form factor. We calculate matrix elements and form factors for the decay  $B \rightarrow K \bar{l} l$  and compare their behavior with those calculated in [8]. In Sec. V we present our numerical results for branching ratios and asymmetry parameters. We plot the  $q^2$ -dependence of the differential decay rate and the longitudinal polarization of the leptons with and without long distance contributions.

## 2 Effective Hamiltonian

The starting point of the description of the rare exclusive decays is the effective Hamiltonian obtained from the SM-diagrams by using the operator product expansion and renormalization group techniques. It allows one to separate the short-distance contributions and isolate them in the Wilson coefficients which can be studied systematically within perturbative QCD. The long-distance contributions are contained in the matrix elements of local operators. Contrary to the short-distance contributions the calculation of such matrix elements requires nonperturbative methods and is therefore model dependent.

We will follow Refs.[7] in writing down the analytical expressions for the effective Hamiltonian and paper [8] in using the numerical values of the input parameters characterizing the short-distance contributions. At the quark level, the rare semileptonic decay  $b \rightarrow s(d)l^+l^-$  can be described in terms of the effective Hamiltonian:

$$H_{\text{eff}} = -\frac{G_F}{\sqrt{2}} \lambda_t \sum_{i=1}^{10} C_i(\mu) Q_i(\mu). \quad (3)$$

where  $\lambda_t \equiv V_{ts(d)}^\dagger V_{tb}$  is the product of CKM elements. For example, the standard set [7] of local operators for  $b \rightarrow sl^+l^-$  transition is written as

$$\begin{aligned} Q_1 &= (\bar{s}_i c_j)_{V-A}, & Q_2 &= (\bar{s} c)_{V-A} (\bar{c} b)_{V-A}, \\ Q_3 &= (\bar{s} b)_{V-A} \sum_q (\bar{q} q)_{V-A}, & Q_4 &= (\bar{s}_i b_j)_{V-A} \sum_q (\bar{q}_j q_i)_{V-A}, \\ Q_5 &= (\bar{s} b)_{V-A} \sum_q (\bar{q} q)_{V+A}, & Q_6 &= (\bar{s}_i b_j)_{V-A} \sum_q (\bar{q}_j q_i)_{V+A}, \\ Q_7 &= \frac{e}{8\pi^2} m_b (\bar{s} \sigma^{\mu\nu} (1 + \gamma_5) b) F_{\mu\nu}, & Q_8 &= \frac{q}{8\pi^2} m_b (\bar{s}_i \sigma^{\mu\nu} (1 + \gamma_5) \mathbf{T}_{ij} b_j) \mathbf{G}_{\mu\nu}, \\ Q_9 &= \frac{e}{8\pi^2} (\bar{s} b)_{V-A} (\bar{l} l)_V, & Q_{10} &= \frac{e}{8\pi^2} (\bar{s} b)_{V-A} (\bar{l} l)_A \end{aligned} \quad (4)$$

where  $\mathbf{G}_{\mu\nu}$  and  $F_{\mu\nu}$  are the gluon and photon field strengths, respectively;  $\mathbf{T}_{ij}$  are the generators of the  $SU(3)$  color group;  $i$  and  $j$  denote color indices (they are omitted in the color-singlet currents). Labels  $(V \pm A)$  stand for  $\gamma^\mu (1 \pm \gamma^5)$ .  $Q_{1,2}$  are current-current operators,  $Q_{3-6}$  are QCD penguin operators,  $Q_{7,8}$  are "magnetic penguin" operators, and  $Q_{9,10}$  are semileptonic electroweak penguin operators. Explicit formulae for the Wilson coefficients  $C_i(\mu)$  obtained in leading logarithmic order are written down in Appendix A.

The effective Hamiltonian leads to the free quark  $b \rightarrow sl^+l^-$ -decay amplitude:

$$\begin{aligned} M(b \rightarrow sl^+l^-) &= \frac{G_F \alpha}{2\sqrt{2}\pi} \lambda_t \left\{ C_9^{\text{eff}} (\bar{s} b)_{V-A} (\bar{l} l)_V + C_{10} (\bar{s} b)_{V-A} (\bar{l} l)_A \right. \\ &\quad \left. - \frac{2m_b}{q^2} C_7^{\text{eff}} (\bar{s} i \sigma^{\mu\nu} (1 + \gamma^5) q^\nu b) (\bar{l} l)_V \right\}. \end{aligned} \quad (5)$$

where  $C_7^{\text{eff}} = C_7 - C_5/3 - C_6$ .

The Wilson coefficient  $C_9^{\text{eff}}$  effectively takes into account, first, the contributions from the four-quark operators  $Q_i$  ( $i = 1, \dots, 6$ ) and, second, the nonperturbative effects coming from the  $c\bar{c}$ -resonance contributions which are as usual parametrized by a Breit-Wigner ansatz [23]:

$$\begin{aligned} C_9^{\text{eff}} &= C_9 + C_0 \left\{ h(\hat{m}_c, s) + \frac{3\pi}{\alpha^2} \kappa \sum_{V_i=\psi(1s),\psi(2s)} \frac{\Gamma(V_i \rightarrow l^+l^-) m_{V_i}}{m_{V_i}^2 - q^2 - im_{V_i}\Gamma_{V_i}} \right\} \\ &- \frac{1}{2} h(1, s) (4C_3 + 4C_4 + 3C_5 + C_6) \\ &- \frac{1}{2} h(0, s) (C_3 + 3C_4) + \frac{2}{9} (3C_3 + C_4 + 3C_5 + C_6) . \end{aligned} \quad (6)$$

where  $C_0 \equiv 3C_1 + C_2 + 3C_3 + C_4 + 3C_5 + C_6$ . Here

$$\begin{aligned} h(\hat{m}_c, s) &= -\frac{8}{9} \ln \frac{m_b}{\mu} - \frac{8}{9} \ln \hat{m}_c + \frac{8}{27} + \frac{4}{9} x \\ &- \frac{2}{9} (2+x) |1-x|^{1/2} \begin{cases} \left( \ln \left| \frac{\sqrt{1-x}+1}{\sqrt{1-x}-1} \right| - i\pi \right), & \text{for } x \equiv \frac{4\hat{m}_c^2}{s} < 1 \\ 2 \arctan \frac{1}{\sqrt{x-1}}, & \text{for } x \equiv \frac{4\hat{m}_c^2}{s} > 1, \end{cases} \\ h(0, s) &= \frac{8}{27} - \frac{8}{9} \ln \frac{m_b}{\mu} - \frac{4}{9} \ln s + \frac{4}{9} i\pi . \end{aligned}$$

where  $\hat{m}_c = m_c/m_B$ ,  $s = q^2/m_B^2$  and  $\kappa = 1/C_0$ .

The relation between the  $\overline{MS}$  b-quark mass  $m_b \equiv m_b(\mu)$  at a scale  $\mu$  and its pole mass  $m_{b,\text{pole}}$  is given by

$$m_b(\mu) = m_{b,\text{pole}} \left\{ 1 - \frac{4}{3} \frac{\alpha_s(\mu)}{\pi} \left[ 1 - \frac{3}{4} \ln \left( \frac{m_{b,\text{pole}}}{\mu^2} \right) \right] \right\} \quad (7)$$

where

$$\alpha_s(\mu) = \frac{4\pi}{\beta_0 \ln \frac{\mu^2}{\Lambda_{QCD}^2}} \left\{ 1 - \frac{\beta_1}{\beta_0^2} \frac{\ln \ln \frac{\mu^2}{\Lambda_{QCD}^2}}{\ln \frac{\mu^2}{\Lambda_{QCD}^2}} \right\} \quad (8)$$

and where  $\beta_0 = 23/3$  and  $\beta_1 = 116/3$ , as is appropriate for five flavors. We will use a scale  $\mu = m_{b,\text{pole}}$  throughout this paper. The numerical values of the input parameters are taken from [8] and the corresponding values of the Wilson coefficients used in the numerical calculations are listed in Table 1.

### 3 $B \rightarrow K\bar{l}l$ and $B_c \rightarrow D(D^*)\bar{l}l$ -decays

#### 3.1 Form factors and differential decay distributions

We specify our choice of the momenta as  $p_1 = p_2 + k_1 + k_2$  with  $p_1^2 = m_1^2$ ,  $p_2^2 = m_2^2$  and  $k_1^2 = k_2^2 = \mu^2$  where  $k_1$  and  $k_2$  are the  $l^+$  and  $l^-$  momenta, and  $m_1$ ,  $m_2$ ,  $\mu$  are the masses of initial meson  $H_{in}$ , final meson  $H_f$  and lepton, respectively.

The matrix elements of the exclusive transitions  $B \rightarrow K\bar{l}l$  and  $B_c \rightarrow D(D^*)\bar{l}l$  are defined by

$$\begin{aligned} M(H_{in} \rightarrow H_f \bar{l}l) &= \frac{G_F}{\sqrt{2}} \cdot \frac{\alpha \lambda_t}{2\pi} \cdot \left\{ C_9^{\text{eff}} < H_f | \bar{s} O^\mu b | H_{in} > \bar{l} \gamma^\mu l \right. \\ &+ C_{10} < H_f | \bar{s} O^\mu b | H_{in} > \bar{l} \gamma^\mu \gamma^5 l \\ &\left. - \frac{2m_b}{q^2} C_7^{\text{eff}} < H_f | \bar{s} i\sigma^{\mu\nu} (1 + \gamma^5) q^\nu b | H_{in} > \bar{l} \gamma^\mu l \right\}. \end{aligned} \quad (9)$$

where  $H_{in} = B$  or  $B_c$ ,  $H_f = K, D$  or  $D^*$ .

We define dimensionless form factors by

$$< K(D)(p_2) | \bar{s}(d) \gamma_\mu b | B(B_c)(p_1) > = F_+(q^2) P_\mu + F_-(q^2) q_\mu, \quad (10)$$

$$\begin{aligned} < K(D)(p_2) | \bar{s}(d) i\sigma_{\mu\nu} q^\nu b | B(B_c)(p_1) > &= -\frac{1}{m_1 + m_2} P_\mu^\perp q^2 F_T(q^2), \\ i < D^*(p_2, \epsilon_2) | \bar{d} O_\mu b | B_c(p_1) &= \frac{1}{m_1 + m_2} \epsilon_2^{\dagger\nu} \\ &\times \{ -g_{\mu\nu} P q A_0(q^2) + P_\mu P_\nu A_+(q^2) + q_\mu P_\nu A_-(q^2) + i\varepsilon_{\mu\nu\alpha\beta} P^\alpha q^\beta V(q^2) \}, \end{aligned}$$

$$\begin{aligned} i < D^*(p_2, \epsilon_2) | \bar{d} i\sigma_{\mu\nu} q^\nu (1 + \gamma_5) b | B_c(p_1) &= \\ &= \epsilon_2^{\dagger\nu} \{ g_{\mu\nu}^\perp P q a_0(q^2) - P_\mu^\perp P_\nu a_+(q^2) - i\varepsilon_{\mu\nu\alpha\beta} P^\alpha q^\beta g(q^2) \} \end{aligned}$$

where  $P = p_1 + p_2$ ,  $q = p_1 - p_2$ ,  $P_\mu^\perp \doteq P_\mu - q_\mu P q / q^2$ ,  $g_{\mu\nu}^\perp \doteq g_{\mu\nu} - q_\mu q_\nu / q^2$ , and  $\epsilon_2^\dagger$  is the polarization four-vector of the  $D^*$ . Since we want to compare our calculations with those in [8] and [17], it is useful to relate our form factors to those used in [8] and [17]. The relations read

$$\begin{aligned} F_+ &= f_+^{\text{Ali}} = F_+^{\text{Geng}} \\ F_- &= -\frac{m_1^2 - m_2^2}{q^2} (f_+ - f_0)^{\text{Ali}} = F_-^{\text{Geng}} \\ F_T &= f_T^{\text{Ali}} = -F_T^{\text{Geng}} \\ A_0 &= \frac{m_1 + m_2}{m_1 - m_2} A_1^{\text{Ali}} = -A_0^{\text{Geng}} \\ A_+ &= A_2^{\text{Ali}} = A_+^{\text{Geng}} \\ A_- &= \frac{2m_2(m_1 + m_2)}{q^2} (A_3 - A_0)^{\text{Ali}} = A_-^{\text{Geng}} \\ V &= V^{\text{Ali}} = -V^{\text{Geng}} \\ a_0 &= T_2^{\text{Ali}} = a_0^{\text{Geng}} \end{aligned}$$

$$\begin{aligned} a_+ &= (T_2 + \frac{q^2}{m_1^2 - m_2^2} T_3)^{\text{Ali}} = -a_+^{\text{Geng}} \\ g &= T_1^{\text{Ali}} = g^{\text{Geng}} \end{aligned}$$

The matrix element in Eq (9) is written as

$$M(B(B_c) \rightarrow K(D^*) \bar{l}l) = \frac{G_F}{\sqrt{2}} \cdot \frac{\alpha \lambda_t}{2\pi} \{ T_1^\mu (\bar{l} \gamma_\mu l) + T_2^\mu (\bar{l} \gamma_\mu \gamma_5 l) \} \quad (11)$$

where the quantities  $T_i^\mu$  are expressed through the form factors and the Wilson coefficients in the following manner:

**(a)**  $B(B_c) \rightarrow K(D) \bar{l}l$ -decay:

$$\begin{aligned} T_i^\mu &= \mathcal{F}_+^{(i)} P^\mu + \mathcal{F}_-^{(i)} q^\mu \quad (i = 1, 2), \quad (12) \\ \mathcal{F}_+^{(1)} &= C_9^{\text{eff}} F_+ + C_7^{\text{eff}} F_T \frac{2m_b}{m_1 + m_2}, \\ \mathcal{F}_-^{(1)} &= C_9^{\text{eff}} F_- - C_7^{\text{eff}} F_T \frac{2m_b}{m_1 + m_2} \frac{Pq}{q^2}, \\ \mathcal{F}_\pm^{(2)} &= C_{10} F_\pm. \end{aligned}$$

**(b)**  $B_c \rightarrow D^* \bar{l}l$ -decay:

$$T_i^\mu = T_i^{\mu\nu} \epsilon_{2\nu}^\dagger, \quad (i = 1, 2), \quad (13)$$

$$\begin{aligned} T_i^{\mu\nu} &= \frac{1}{m_1 + m_2} \{ -Pq g^{\mu\nu} A_0^{(i)} + P^\mu P^\nu A_+^{(i)} + q^\mu P^\nu A_-^{(i)} + i\varepsilon^{\mu\nu\alpha\beta} P_\alpha q_\beta V^{(i)} \} \\ V^{(1)} &= C_9^{\text{eff}} V + C_7^{\text{eff}} g \frac{2m_b(m_1 + m_2)}{q^2}, \\ A_0^{(1)} &= C_9^{\text{eff}} A_0 + C_7^{\text{eff}} a_0 \frac{2m_b(m_1 + m_2)}{q^2}, \\ A_+^{(1)} &= C_9^{\text{eff}} A_+ + C_7^{\text{eff}} a_+ \frac{2m_b(m_1 + m_2)}{q^2}, \\ A_-^{(1)} &= C_9^{\text{eff}} A_- + C_7^{\text{eff}} (a_0 - a_+) \frac{2m_b(m_1 + m_2)}{q^2} \frac{Pq}{q^2}, \\ V^{(2)} &= C_{10} V, \quad A_0^{(2)} = C_{10} A_0, \quad A_\pm^{(2)} = C_{10} A_\pm. \end{aligned}$$

Let us first consider the polar angle decay distribution differential in the momentum transfer squared  $q^2$ . The polar angle is defined by the angle between  $\mathbf{q} = \mathbf{p}_1 - \mathbf{p}_2$  and  $\mathbf{k}_1$  ( $l^+l^-$  rest frame) as shown in Fig. 1. One has

$$\frac{d^2\Gamma}{dq^2 d\cos\theta} = \frac{|\mathbf{p}_2| v}{(2\pi)^3 4 m_1^3} \cdot \frac{1}{8} \sum_{\text{pol}} |M|^2 = \frac{G_F^2}{(2\pi)^3} \left( \frac{\alpha |\lambda_t|}{2\pi} \right)^2 \frac{|\mathbf{p}_2| v}{8m_1^2} \quad (14)$$

$$\begin{aligned}
& \times \frac{1}{8} \left\{ H_{11}^{\mu\nu} \cdot \text{tr}[\gamma_\mu (\not{k}_1 - \mu) \gamma_\nu (\not{k}_2 + \mu)] \right. \\
& + H_{22}^{\mu\nu} \cdot \text{tr}[\gamma_\mu \gamma_5 (\not{k}_1 - \mu) \gamma_\nu \gamma_5 (\not{k}_2 + \mu)] \\
& + H_{12}^{\mu\nu} \cdot \text{tr}[\gamma_\mu (\not{k}_1 - \mu) \gamma_\nu \gamma_5 (\not{k}_2 + \mu)] \\
& \left. + H_{21}^{\mu\nu} \cdot \text{tr}[\gamma_\mu \gamma_5 (\not{k}_1 - \mu) \gamma_\nu (\not{k}_2 + \mu)] \right\} \\
& = \frac{G_F^2}{(2\pi)^3} \left( \frac{\alpha |\lambda_t|}{2\pi} \right)^2 \frac{|\mathbf{p}_2| v}{8m_1^2} \cdot \frac{1}{2} \left\{ L_{\mu\nu}^{(1)} \cdot (H_{11}^{\mu\nu} + H_{22}^{\mu\nu}) \right. \\
& \left. - \frac{1}{2} L_{\mu\nu}^{(2)} \cdot (q^2 H_{11}^{\mu\nu} + (q^2 - 4\mu^2) H_{22}^{\mu\nu}) + L_{\mu\nu}^{(3)} \cdot (H_{12}^{\mu\nu} + H_{21}^{\mu\nu}) \right\}
\end{aligned}$$

where  $|\mathbf{p}_2| = \lambda^{1/2}(m_1^2, m_2^2, q^2)/2m_1$  is the momentum of the  $K(D^*)$ -meson and  $v = \sqrt{1 - 4\mu^2/q^2}$  is the lepton velocity both given in the  $B(B_c)$ -rest frame. We have introduced lepton and hadron tensors as

$$\begin{aligned}
L_{\mu\nu}^{(1)} &= k_{1\mu} k_{2\nu} + k_{2\mu} k_{1\nu}, & L_{\mu\nu}^{(2)} &= g_{\mu\nu}, & L_{\mu\nu}^{(3)} &= i\varepsilon_{\mu\nu\alpha\beta} k_1^\alpha k_2^\beta, \\
H_{ij}^{\mu\nu} &= T_i^\mu T_j^\nu.
\end{aligned} \tag{15}$$

### 3.2 Helicity amplitudes and two-fold distributions

The Lorentz contractions in Eq. (14) can be evaluated in terms of helicity amplitudes as described in [24]. First, we define an orthonormal and complete helicity basis  $\epsilon^\mu(m)$  with the three spin 1 components orthogonal to the momentum transfer  $q^\mu$ , i.e.  $\epsilon^\mu(m)q_\mu = 0$  for  $m = \pm, 0$ , and the spin 0 (time)-component  $m = t$  with  $\epsilon^\mu(t) = q^\mu/\sqrt{q^2}$ .

The orthonormality and completeness properties read

$$\begin{aligned}
\epsilon_\mu^\dagger(m) \epsilon^\mu(n) &= g_{mn} \quad (m, n = t, \pm, 0), \\
\epsilon_\mu(m) \epsilon_\nu^\dagger(n) g_{mn} &= g_{\mu\nu}
\end{aligned} \tag{16}$$

with  $g_{mn} = \text{diag}(+, -, -, -)$ . We include the time component polarization vector  $\epsilon^\mu(t)$  in the set because we want to discuss lepton mass effects in the following.

Using the completeness property we rewrite the contraction of the lepton and hadron tensors in Eq. (14) according to

$$\begin{aligned}
L^{(k)\mu\nu} H_{\mu\nu}^{ij} &= L_{\mu'\nu'}^{(k)} \epsilon^{\mu'}(m) \epsilon^{\dagger\mu}(m') g_{mm'} \epsilon^{\dagger\nu'}(n) \epsilon^\nu(n') g_{nn'} H_{\mu\nu}^{ij} \\
&= L^{(k)}(m, n) g_{mm'} g_{nn'} H^{ij}(m', n')
\end{aligned} \tag{17}$$

where we have introduced the lepton and hadron tensors in the space of the helicity components

$$L^{(k)}(m, n) = \epsilon^\mu(m) \epsilon^{\dagger\nu}(n) L_{\mu\nu}^{(k)}, \quad H^{ij}(m, n) = \epsilon^{\dagger\mu}(m) \epsilon^\nu(n) H_{\mu\nu}^{ij}. \quad (18)$$

The point is that the two tensors can be evaluated in two different Lorentz systems. The lepton tensors  $L^{(k)}(m, n)$  will be evaluated in the  $\bar{l}l$ -CM system whereas the hadron tensors  $H^{ij}(m, n)$  will be evaluated in the  $B(B_c)$  rest system.

In the  $B(B_c)$  rest frame one has

$$\begin{aligned} p_1^\mu &= (m_1, 0, 0, 0), \\ p_2^\mu &= (E_2, 0, 0, -|\mathbf{p}_2|), \\ q^\mu &= (q_0, 0, 0, |\mathbf{p}_2|), \end{aligned} \quad (19)$$

where  $E_2 = (m_1^2 + m_2^2 - q^2)/2m_1$  and  $q_0 = (m_1^2 - m_2^2 + q^2)/2m_1$ . In the  $B(B_c)$ -rest frame the polarization vectors of the effective current read

$$\begin{aligned} \epsilon^\mu(t) &= \frac{1}{\sqrt{q^2}} (q_0, 0, 0, |\mathbf{p}_2|), \\ \epsilon^\mu(\pm) &= \frac{1}{\sqrt{2}} (0, \mp 1, -i, 0), \\ \epsilon^\mu(0) &= \frac{1}{\sqrt{q^2}} (|\mathbf{p}_2|, 0, 0, q_0). \end{aligned} \quad (20)$$

Using this basis one can express the components of the hadronic tensors through the invariant form factors defined in Eq. (10).

(a)  $B(B_c) \rightarrow K(D)$  transition:

$$H^{ij}(m, n) = (\epsilon^{\dagger\mu}(m) T_\mu^i) \cdot (\epsilon^{\dagger\nu}(n) T_\nu^j)^\dagger \equiv H^i(m) H^{\dagger j}(n) \quad (21)$$

The helicity form factors  $H^i(m)$  are given in terms of the invariant form factors. One has

$$\begin{aligned} H^i(t) &= \frac{1}{\sqrt{q^2}} (Pq \mathcal{F}_+^i + q^2 \mathcal{F}_-^i), \\ H^i(\pm) &= 0, \\ H^i(0) &= \frac{2m_1|\mathbf{p}_2|}{\sqrt{q^2}} \mathcal{F}_+^i. \end{aligned} \quad (22)$$

(b)  $B_c \rightarrow D^*$  transition:

$$\begin{aligned}
 H^{ij}(m, n) &= \epsilon^{\dagger\mu}(m)\epsilon^\nu(n)H_{\mu\nu}^{ij} = \epsilon^{\dagger\mu}(m)\epsilon^\nu(n)T_{\mu\alpha}^i \left( -g^{\alpha\beta} + \frac{p_2^\alpha p_2^\beta}{m_2^2} \right) T_{\beta\nu}^j \\
 &= \epsilon^{\dagger\mu}(m)\epsilon^\nu(n)T_{\mu\alpha}^i \epsilon_2^{\dagger\alpha}(r)\epsilon_2^\beta(s)\delta_{rs}T_{\beta\nu}^j \\
 &= \epsilon^{\dagger\mu}(m)\epsilon_2^{\dagger\alpha}(r)T_{\mu\alpha}^i \cdot \left( \epsilon^{\dagger\nu}(n)\epsilon_2^{\dagger\beta}(s)T_{\nu\beta}^j \right)^\dagger \delta_{rs} = H^i(m)H^{\dagger j}(n).
 \end{aligned} \tag{23}$$

From angular momentum conservation one has  $r = m$  and  $s = n$  for  $m, n = \pm, 0$  and  $r, s = 0$  for  $m, n = t$ . For further evaluation one needs to specify the helicity components  $\epsilon_2(m)$  ( $m = \pm, 0$ ) of the polarization vector of the  $D^*$ . They read

$$\begin{aligned}
 \epsilon_2^\mu(\pm) &= \frac{1}{\sqrt{2}}(0, \pm 1, -i, 0), \\
 \epsilon_2^\mu(0) &= \frac{1}{m_2}(|\mathbf{p}_2|, 0, 0, -E_2).
 \end{aligned} \tag{24}$$

They satisfy the orthonormality and completeness properties:

$$\begin{aligned}
 \epsilon_2^{\dagger\mu}(r)\epsilon_{2\mu}(s) &= -\delta_{rs}, \\
 \epsilon_{2\mu}(r)\epsilon_{2\nu}^\dagger(s)\delta_{rs} &= -g_{\mu\nu} + \frac{p_{2\mu}p_{2\nu}}{m_2^2}.
 \end{aligned} \tag{25}$$

Finally one obtains the non-zero components of the hadron tensors

$$\begin{aligned}
 H^i(t) &= \epsilon^{\dagger\mu}(t)\epsilon_2^{\dagger\alpha}(0)T_{\mu\alpha}^i = \frac{1}{m_1 + m_2} \frac{m_1 |\mathbf{p}_2|}{m_2 \sqrt{q^2}} (Pq(-A_0^i + A_+^i) + q^2 A_-^i), \\
 H^i(\pm) &= \epsilon^{\dagger\mu}(\pm)\epsilon_2^{\dagger\alpha}(\pm)T_{\mu\alpha}^i = \frac{1}{m_1 + m_2} (-Pq A_0^i \pm 2m_1 |\mathbf{p}_2| V^i), \\
 H^i(0) &= \epsilon^{\dagger\mu}(0)\epsilon_2^{\dagger\alpha}(0)T_{\mu\alpha}^i \\
 &= \frac{1}{m_1 + m_2} \frac{1}{2m_2 \sqrt{q^2}} (-Pq(m_1^2 + m_2^2 - q^2) A_0^i + 4m_1^2 |\mathbf{p}_2|^2 A_+^i).
 \end{aligned} \tag{26}$$

The lepton tensors  $L^{(k)}(m, n)$  are evaluated in the  $\bar{l}l$ -CM system  $\mathbf{k}_1 + \mathbf{k}_2 = 0$ . One has (see Fig. 1)

$$\begin{aligned}
 q^\mu &= (\sqrt{q^2}, 0, 0, 0), \\
 k_1^\mu &= (E_1, |\mathbf{k}_1| \sin \theta \cos \chi, |\mathbf{k}_1| \sin \theta \sin \chi, |\mathbf{k}_1| \cos \theta), \\
 k_2^\mu &= (E_1, -|\mathbf{k}_1| \sin \theta \cos \chi, -|\mathbf{k}_1| \sin \theta \sin \chi, -|\mathbf{k}_1| \cos \theta),
 \end{aligned} \tag{27}$$

with  $E_1 = \sqrt{q^2}/2$  and  $|\mathbf{k}_1| = \sqrt{q^2 - 4\mu^2}/2$ . The longitudinal and time component polarization vectors in the  $\bar{l}l$  rest frame can be read off from Eq. (20) and are given by  $\epsilon^\mu(0) = (0, 0, 0, 1)$  and  $\epsilon(t) = (1, 0, 0, 0)$  whereas the transverse parts remain unchanged from Eq. (20).

The differential  $(q^2, \cos \theta)$  distribution finally reads

$$\begin{aligned} \frac{d\Gamma(H_{in} \rightarrow H_f \bar{l}l)}{dq^2 d(\cos \theta)} &= \frac{3}{8} (1 + \cos^2 \theta) \cdot \frac{1}{2} \left( \frac{d\Gamma_U^{11}}{dq^2} + \frac{d\Gamma_U^{22}}{dq^2} \right) \\ &+ \frac{3}{4} \sin^2 \theta \cdot \frac{1}{2} \left( \frac{d\Gamma_L^{11}}{dq^2} + \frac{d\Gamma_L^{22}}{dq^2} \right) \\ &- v \cdot \frac{3}{4} \cos \theta \cdot \frac{d\Gamma_P^{12}}{dq^2} \\ &+ \frac{3}{4} \sin^2 \theta \cdot \frac{1}{2} \frac{d\tilde{\Gamma}_U^{11}}{dq^2} - \frac{3}{8} (1 + \cos^2 \theta) \cdot \frac{d\tilde{\Gamma}_U^{22}}{dq^2} \\ &+ \frac{3}{2} \cos^2 \theta \cdot \frac{1}{2} \frac{d\tilde{\Gamma}_L^{11}}{dq^2} - \frac{3}{4} \sin^2 \theta \cdot \frac{d\tilde{\Gamma}_L^{22}}{dq^2} + \frac{1}{4} \frac{d\tilde{\Gamma}_S^{22}}{dq^2}. \end{aligned} \quad (28)$$

Integrating over  $\cos \theta$  one obtains

$$\begin{aligned} \frac{d\Gamma(H_{in} \rightarrow H_f \bar{l}l)}{dq^2} &= \frac{1}{2} \left( \frac{d\Gamma_U^{11}}{dq^2} + \frac{d\Gamma_U^{22}}{dq^2} + \frac{d\Gamma_L^{11}}{dq^2} + \frac{d\Gamma_L^{22}}{dq^2} \right) \\ &+ \frac{1}{2} \frac{d\tilde{\Gamma}_U^{11}}{dq^2} - \frac{d\tilde{\Gamma}_U^{22}}{dq^2} + \frac{1}{2} \frac{d\tilde{\Gamma}_L^{11}}{dq^2} - \frac{d\tilde{\Gamma}_L^{22}}{dq^2} + \frac{1}{2} \frac{d\tilde{\Gamma}_S^{22}}{dq^2}, \end{aligned} \quad (29)$$

where the partial helicity rates  $d\Gamma_X^{ij}/dq^2$  and  $d\tilde{\Gamma}_X^{ij}/dq^2$  ( $X = U, L, P, S$ ;  $i, j = 1, 2$ ) are defined as

$$\begin{aligned} \frac{d\Gamma_{X_{ij}}}{dq^2} &= \frac{G_F^2}{(2\pi)^3} \left( \frac{\alpha |\lambda_t|}{2\pi} \right)^2 \frac{|\mathbf{p}_2| q^2 v}{12 m_1^2} H_X^{ij}, \\ \frac{d\tilde{\Gamma}_{X_{ij}}}{dq^2} &= \frac{2\mu^2}{q^2} \frac{d\Gamma_X^{ij}}{dq^2}. \end{aligned} \quad (30)$$

The relevant bilinear combinations of the helicity amplitudes are defined in Table 2.

To check our calculation we give the corresponding expression for the differential decay rate used in [8] and [17]:

$$\frac{d\Gamma(B \rightarrow Kl^+l^-)}{ds} = \frac{G_F^2 |\lambda_t|^2 m_1^5 \alpha^2}{3 \cdot 2^9 \pi^5} v \phi_H^{\frac{1}{2}} \left[ \left( 1 + \frac{2t}{s} \right) \phi_H \alpha_2 + 12t \beta_2 \right], \quad (31)$$

with  $s = q^2/m_1^2$  and  $t = \mu^2/m_1^2$  and the expressions of  $\phi_H$ ,  $\alpha_i$ ,  $\beta_i$ ,  $\delta$  ( $i=1,2,3$ ) and  $\delta$  are given in Appendix B. We find complete agreement with the decay distributions given in [8] and [17].

### 3.3 The four-fold angle distribution in the cascade decay $B_c \rightarrow D^*(\rightarrow D\pi) \bar{l}l$ .

The lepton-hadron correlation function  $L_{\mu\nu} H^{\mu\nu}$  reveals even more structure when one uses the cascade decay  $B_c \rightarrow D^*(\rightarrow D\pi) \bar{l}l$  to analyze the polarization of the  $D^*$ . The hadron tensor now reads

$$H_{\mu\nu}^{ij} = T_{\mu\alpha}^i (T_{\nu\beta}^j)^\dagger \frac{3}{2|\mathbf{p}_3|} \text{Br}(D^* \rightarrow D\pi) p_{3\alpha'} p_{3\beta'} S^{\alpha\alpha'}(p_2) S^{\beta\beta'}(p_2) \quad (32)$$

where  $S^{\alpha\alpha'}(p_2) = -g^{\alpha\alpha'} + p_2^\alpha p_2^{\alpha'}/m_2^2$  is the standard spin 1 tensor,  $p_2 = p_3 + p_4$ ,  $p_3^2 = m_D^2$ ,  $p_4^2 = m_\pi^2$ , and  $p_3$  and  $p_4$  are the momenta of the  $D$  and the  $\pi$ , respectively. The relative configuration of the  $(D, \pi)$ - and  $(\bar{l}l)$ -planes is shown in Fig. 1.

In the rest frame of the  $D^*$  one has

$$\begin{aligned} p_2^\mu &= (m_{D^*}, \mathbf{0}), \\ p_3^\mu &= (E_D, |\mathbf{p}_3| \sin \theta^*, 0, -|\mathbf{p}_3| \cos \theta^*), \\ p_4^\mu &= (E_\pi, -|\mathbf{p}_3| \sin \theta^*, 0, |\mathbf{p}_3| \cos \theta^*), \\ |\mathbf{p}_3| &= \lambda^{1/2}(m_{D^*}^2, m_D^2, m_\pi^2)/(2m_{D^*}). \end{aligned} \quad (33)$$

Without loss of generality we set the azimuthal angle  $\chi^*$  of the  $(D, \pi)$ -plane to zero. According to Eq. (24) the rest frame polarization vectors of the  $D^*$  are given by

$$\begin{aligned} \epsilon_2^\mu(\pm) &= \frac{1}{\sqrt{2}}(0, \pm 1, -i, 0), \\ \epsilon_2^\mu(0) &= (0, 0, 0, -1). \end{aligned} \quad (34)$$

The spin 1 tensor  $S^{\alpha\alpha'}(p_2)$  is then written as

$$S^{\alpha\alpha'}(p_2) = -g^{\alpha\alpha'} + \frac{p_2^\alpha p_2^{\alpha'}}{m_2^2} = \sum_{m=\pm,0} \epsilon_2^\alpha(m) \epsilon_2^{\dagger\alpha'}(m). \quad (35)$$

Following basically the same trick as in Eq. (17) the contraction of the lepton and hadron tensors may be written through helicity components as

$$\begin{aligned} L^{(k)\mu\nu} H_{\mu\nu}^{ij} &= \epsilon^{\mu'}(m) \epsilon^{\dagger\nu'}(n) L_{\mu'\nu'}^k g_{mn'} g_{nn'} \epsilon^{\dagger\mu}(m') \epsilon^\nu(n') H_{\mu\nu}^{ij} \\ &= L^k(m, n) g_{mm'} g_{nn'} \left( \epsilon^{\dagger\mu}(m') \epsilon_2^{\dagger\alpha}(r) T_{\mu\alpha}^i \right) \left( \epsilon^{\dagger\nu}(n') \epsilon_2^{\dagger\alpha}(s) T_{\nu\beta}^j \right)^\dagger \\ &\times p_3 \epsilon_2(r) \cdot p_3 \epsilon_2^\dagger(s) \frac{3 \text{Br}(D^* \rightarrow D\pi)}{2|\mathbf{p}_3|} \\ &= \frac{3 \text{Br}(D^* \rightarrow D\pi)}{2|\mathbf{p}_3|} \left( L^k(t, t) |H^{ij}(t)|^2 \cdot (p_3 \epsilon_2^\dagger(0))^2 \right. \\ &+ \sum_{m,n=\pm,0} L^k(m, n) H^i(m) H^{\dagger j}(n) \cdot p_3 \epsilon_2(m) \cdot p_3 \epsilon_2^\dagger(n) \\ &- \sum_{n=\pm,0} L^k(t, n) H^i(t) H^{\dagger j}(n) \cdot p_3 \epsilon_2(0) \cdot p_3 \epsilon_2^\dagger(n) \\ &\left. - \sum_{m=\pm,0} L^k(m, t) H^i(m) H^{\dagger j}(t) \cdot p_3 \epsilon_2(m) \cdot p_3 \epsilon_2^\dagger(0) \right). \end{aligned} \quad (36)$$

Using these results one obtains the full four-fold angular decay distribution

$$\begin{aligned}
 & \frac{d\Gamma(B_c \rightarrow D^*(\rightarrow D\pi)\bar{l}l)}{dq^2 d\cos\theta d(\chi/2\pi) d\cos\theta^*} = \text{Br}(D^* \rightarrow D\pi) \\
 & \times \left\{ \frac{3}{8} (1 + \cos^2\theta) \cdot \frac{3}{4} \sin^2\theta^* \cdot \frac{1}{2} \left( \frac{d\Gamma_U^{11}}{dq^2} + \frac{d\Gamma_U^{22}}{dq^2} \right) \right. \\
 & + \frac{3}{4} \sin^2\theta \cdot \frac{3}{2} \cos^2\theta^* \cdot \frac{1}{2} \left( \frac{d\Gamma_L^{11}}{dq^2} + \frac{d\Gamma_L^{22}}{dq^2} \right) \\
 & - \frac{3}{4} \sin^2\theta \cdot \cos 2\chi \cdot \frac{3}{4} \sin^2\theta^* \cdot \frac{1}{2} \left( \frac{d\Gamma_T^{11}}{dq^2} + \frac{d\Gamma_T^{22}}{dq^2} \right) \\
 & + \frac{9}{16} \sin 2\theta \cdot \cos \chi \cdot \sin 2\theta^* \cdot \frac{1}{2} \left( \frac{d\Gamma_I^{11}}{dq^2} + \frac{d\Gamma_I^{22}}{dq^2} \right) \\
 & + v \left[ -\frac{3}{4} \cos\theta \cdot \frac{3}{4} \sin^2\theta^* \cdot \frac{d\Gamma_P^{12}}{dq^2} \right. \\
 & - \frac{9}{8} \sin\theta \cdot \cos\chi \cdot \sin 2\theta^* \cdot \frac{1}{2} \left( \frac{d\Gamma_A^{12}}{dq^2} + \frac{d\Gamma_A^{21}}{dq^2} \right) \\
 & + \frac{9}{16} \sin\theta \cdot \sin\chi \cdot \sin 2\theta^* \cdot \left( \frac{d\Gamma_{II}^{12}}{dq^2} + \frac{d\Gamma_{II}^{21}}{dq^2} \right) \\
 & - \frac{9}{32} \sin 2\theta \cdot \sin\chi \cdot \sin 2\theta^* \cdot \left( \frac{d\Gamma_{IA}^{11}}{dq^2} + \frac{d\Gamma_{IA}^{22}}{dq^2} \right) \\
 & + \frac{9}{32} \sin^2\theta \cdot \sin 2\chi \cdot \sin^2\theta^* \cdot \left( \frac{d\Gamma_{IT}^{11}}{dq^2} + \frac{d\Gamma_{IT}^{22}}{dq^2} \right) \\
 & + \frac{3}{4} \sin^2\theta \cdot \frac{3}{4} \sin^2\theta^* \cdot \frac{1}{2} \cdot \frac{d\tilde{\Gamma}_U^{11}}{dq^2} - \frac{3}{8} (1 + \cos^2\theta) \cdot \frac{3}{4} \sin^2\theta^* \cdot \frac{d\tilde{\Gamma}_U^{22}}{dq^2} \\
 & + \frac{3}{2} \cos^2\theta \cdot \frac{3}{2} \cos^2\theta^* \cdot \frac{1}{2} \cdot \frac{d\tilde{\Gamma}_L^{11}}{dq^2} - \frac{3}{4} \sin^2\theta \cdot \frac{3}{2} \cos^2\theta^* \cdot \frac{d\tilde{\Gamma}_L^{22}}{dq^2} \\
 & + \frac{3}{4} \sin^2\theta \cdot \cos 2\chi \cdot \frac{3}{4} \sin^2\theta^* \cdot \left( \frac{d\tilde{\Gamma}_T^{11}}{dq^2} + \frac{d\tilde{\Gamma}_T^{22}}{dq^2} \right) \\
 & - \frac{9}{8} \sin 2\theta \cdot \cos\chi \cdot \sin 2\theta^* \cdot \frac{1}{2} \left( \frac{d\tilde{\Gamma}_I^{11}}{dq^2} + \frac{d\tilde{\Gamma}_I^{22}}{dq^2} \right) + \frac{3}{2} \cos^2\theta^* \cdot \frac{1}{4} \frac{d\tilde{\Gamma}_S^{22}}{dq^2} \\
 & + \frac{9}{16} \sin 2\theta \cdot \sin\chi \cdot \sin 2\theta^* \cdot \left( \frac{d\tilde{\Gamma}_{IA}^{11}}{dq^2} + \frac{d\tilde{\Gamma}_{IA}^{22}}{dq^2} \right) \\
 & \left. - \frac{9}{16} \sin^2\theta \cdot \sin 2\chi \cdot \sin^2\theta^* \cdot \left( \frac{d\tilde{\Gamma}_{IT}^{11}}{dq^2} + \frac{d\tilde{\Gamma}_{IT}^{22}}{dq^2} \right) \right\}
 \end{aligned} \tag{37}$$

Integrating Eq. (37) over  $\cos\theta^*$  and  $\chi$  one recovers the two-fold  $(q^2, \cos\theta)$  distribution of Eq. (28). Note that a similar four-fold distribution has also been obtained in Refs.([14],[25]-[28]) using, however, the zero lepton mass approximation. If there are sufficient data one can attempt to fit them to the full four-fold decay distribution and thereby extract the values of the coefficient functions

$d\Gamma_X/dq^2$  and, in the case  $l = \tau$  the coefficient functions  $d\tilde{\Gamma}_X/dq^2$ . Instead of considering the full four-fold decay distribution one can analyze single angle distributions by integrating out two of the remaining angles as e.g. discussed in Sec.3.2 Observables related to single angle distributions will be discussed in the next subsection.

### 3.4 Physical observables

The four-fold distribution Eq. (37) allows one to define a number of physical observables which can be measured experimentally. An asymmetry parameter  $\alpha_{\theta^*}$  is defined from the angular distribution  $W(\cos^2 \theta^*) = 1 + \alpha_{\theta^*} \cos^2 \theta^*$ . Integrating Eq. (37) over  $\cos \theta$  and  $\chi$  one finds

$$\alpha_{\theta^*} = \frac{-(U^{11} + U^{22}) + 2(L^{11} + L^{22}) - \tilde{U}^{11} + 2\tilde{U}^{22} + 2(\tilde{L}^{11} - 2\tilde{L}^{22}) + 2\tilde{S}^{22}}{U^{11} + U^{22} + \tilde{U}^{11} - 2\tilde{U}^{22}} \quad (38)$$

By integrating over  $\cos \theta^*$  and  $\chi$  one can define two asymmetry parameters  $\alpha'_\theta$  and  $\alpha_\theta$  according to the angular distribution  $W(\cos^2 \theta) = 1 + \alpha'_\theta \cos \theta + \alpha_\theta \cos^2 \theta$ . One has

$$\alpha'_\theta = \frac{-4vP^{12}}{U^{11} + U^{22} + 2(L^{11} + L^{22}) + 2(\tilde{U}^{11} - \tilde{U}^{22} - 2\tilde{L}^{22} + (2/3)\tilde{S}^{22})}, \quad (39)$$

$$\alpha_\theta = \frac{U^{11} + U^{22} - 2(L^{11} + L^{22}) - 2(\tilde{U}^{11} + \tilde{U}^{22}) + 4(\tilde{L}^{11} + \tilde{L}^{22})}{U^{11} + U^{22} + 2(L^{11} + L^{22}) + 2(\tilde{U}^{11} - \tilde{U}^{22} - 2\tilde{L}^{22} + (2/3)\tilde{S}^{22})}. \quad (40)$$

An azimuthal asymmetry parameter  $\beta$  can be defined from the  $\chi$ -distribution  $W(\chi) = 1 + \beta \cos 2\chi$ . The azimuthal  $\chi$ -distribution is obtained by integrating over  $\cos \theta$  and  $\cos \theta^*$ . One has

$$\beta = \frac{-(T^{11} + T^{22}) + 2(\tilde{T}^{11} + \tilde{T}^{22})}{U^{11} + U^{22} + L^{11} + L^{22} + \tilde{U}^{11} - 2\tilde{U}^{22} + \tilde{L}^{11} - 2\tilde{L}^{22} + \tilde{S}^{22}}. \quad (41)$$

A second strategy is to define suitable asymmetry ratios that project out the partial rates from Eq. (37). Let us consider the following four asymmetry ratios which project out the contributions of the parity conserving partial rates  $\Gamma_T$  and  $\Gamma_I$  and the parity violating partial decay rates  $\Gamma_P$  and  $\Gamma_A$ . One has

$$\Gamma_T : \quad A_T = \frac{d\Gamma(\chi) - d\Gamma(\chi + \pi/2) + d\Gamma(\chi + \pi) - d\Gamma(\chi + 3\pi/2)}{d\Gamma(\chi) + d\Gamma(\chi + \pi/2) + d\Gamma(\chi + \pi) + d\Gamma(\chi + 3\pi/2)} \quad (42)$$

where  $-\pi/4 \leq \chi \leq \pi/4$ .

$$\Gamma_A : \quad A_I = N_I/D_I, \quad (43)$$

$$N_I = d\Gamma(\theta, \theta^*, \chi) - d\Gamma(\theta, \theta^*, \chi + \pi)$$

$$\begin{aligned}
& - d\Gamma(\theta, \pi - \theta^*, \chi) + d\Gamma(\theta, \pi - \theta^*, \chi + \pi) \\
& - d\Gamma(\pi - \theta, \theta^*, \chi) + d\Gamma(\pi - \theta, \theta^*, \chi + \pi) \\
& + d\Gamma(\pi - \theta, \pi - \theta^*, \chi) - d\Gamma(\pi - \theta, \pi - \theta^*, \chi + \pi),
\end{aligned}$$

$$0 \leq \theta^* \leq \frac{\pi}{2}, \quad \frac{\pi}{2} \leq \theta \leq \pi, \quad -\frac{\pi}{2} \leq \chi \leq \frac{\pi}{2}.$$

The denominator  $D_I$  is given by the same expression with plus signs everywhere.

$$\Gamma_P : \quad A_{FB} = \frac{d\Gamma(\theta) - d\Gamma(\pi - \theta)}{d\Gamma(\theta) + d\Gamma(\pi - \theta)}, \quad \frac{\pi}{2} \leq \theta \leq \pi, \quad (44)$$

$$\begin{aligned}
\Gamma_A : A_A = & \frac{d\Gamma(\theta^*, \chi) - d\Gamma(\theta^*, \chi + \pi) - d\Gamma(\pi - \theta^*, \chi) + d\Gamma(\pi - \theta^*, \chi + \pi)}{d\Gamma(\theta^*, \chi) + d\Gamma(\theta^*, \chi + \pi) + d\Gamma(\pi - \theta^*, \chi) + d\Gamma(\pi - \theta^*, \chi + \pi)}, \\
& 0 \leq \theta^* \leq \frac{\pi}{2}, \quad -\frac{\pi}{2} \leq \chi \leq \frac{\pi}{2}.
\end{aligned} \quad (45)$$

We have used a notation where the angles that do not appear in the arguments of the differential rates  $d\Gamma$  have been integrated out over their physical ranges ( $0 \leq \theta(\theta^*) \leq \pi$ ,  $0 \leq \chi \leq 2\pi$ ). Integrating over the remaining variables (numerator and denominator separately!) we finally obtain

$$\langle A_T \rangle = \frac{2}{\pi} \frac{-(1/2)(T^{11} + T^{22}) + \tilde{T}^{11} + \tilde{T}^{22}}{\Gamma}, \quad (46)$$

$$\langle A_I \rangle = \frac{2}{\pi} \frac{(1/2)(I^{11} + I^{22}) - \tilde{I}^{11} - \tilde{I}^{22}}{\Gamma}, \quad (47)$$

$$\langle A_{FB} \rangle = \frac{3v}{4} \frac{P^{12}}{\Gamma}, \quad (48)$$

$$\langle A_A \rangle = \frac{3v}{4} \frac{A^{12} + A^{21}}{\Gamma}. \quad (49)$$

### 3.5 Longitudinal polarization of the lepton in $B \rightarrow K\bar{l}l$ -decay.

Our aim is to study lepton polarization effects in  $B \rightarrow K\bar{l}l$ -decay. The longitudinal polarization of the final lepton  $l^-(k_2)$  is defined by

$$P^{(l)} = \frac{d\Gamma(s_2)/dq^2 - d\Gamma(-s_2)/dq^2}{d\Gamma(s_2)/dq^2 + d\Gamma(-s_2)/dq^2} \quad (50)$$

where the longitudinal component of the rest frame polarization vector of the  $l^-(k_2)$  is given by

$$s_2 = \left( 0, \frac{\mathbf{k}_2}{|\mathbf{k}_2|} \right). \quad (51)$$

Contrary to previous studies of the longitudinal polarization of the lepton, where the longitudinal polarization was studied in the B rest frame, we will calculate this quantity in the  $\bar{l}l$ -CM frame. The longitudinal polarization vector  $s_2$  is boosted to the moving frame by a Lorentz transformation. One obtains

$$s_{2,CM} = \left( \frac{|\mathbf{k}_2|}{\mu}, \frac{E_2}{\mu} \frac{\mathbf{k}_2}{|\mathbf{k}_2|} \right). \quad (52)$$

The quantity  $d\Gamma(s_2)/dq^2$  in Eq. (50) may be obtained from Eq. (14) by the replacement

$$(\not{k}_2 + \mu) \rightarrow \frac{1}{2}(1 + \gamma_5) \not{s}_2 (\not{k}_2 + \mu).$$

Integrating the numerator and denominator in Eq. (50) over  $\cos\theta$ , one finds

$$P^{(l)} = \frac{v (dU^{12} + d\tilde{U}^{12})}{d\Gamma} \quad (53)$$

where we have adopted a short hand notation  $U := \Gamma_U$ ,  $\tilde{U} := \tilde{\Gamma}_U$ , etc.. Because of CP-invariance and because the longitudinal polarization is a pseudoscalar quantity, the longitudinal polarization of the antilepton is equal and opposite to the longitudinal polarization of the lepton, i.e.  $P^{(l)}(l^+) = -P^{(l)}(l^-)$ .

#### 4 Model form factors

We will employ the relativistic constituent quark model [18, 19] to calculate the form factors relevant to the decays  $B \rightarrow K\bar{l}l$  and  $B_c \rightarrow D(D^*)\bar{l}l$ . This model is based on an effective interaction Lagrangian which describes the coupling between hadrons and their constituent quarks.

For example, the coupling of the meson  $H$  to its constituent quarks  $q_1$  and  $\bar{q}_2$  is given by the Lagrangian

$$\mathcal{L}_{\text{int}}(x) = g_H H(x) \int dx_1 \int dx_2 F_H(x, x_1, x_2) \bar{q}(x_1) \Gamma_H \lambda_H q(x_2). \quad (54)$$

Here,  $\lambda_H$  and  $\Gamma_H$  are Gell-Mann and Dirac matrices which entail the flavor and spin quantum numbers of the meson field  $H(x)$ . The function  $F_H$  is related to the scalar part of the Bethe-Salpeter amplitude and characterizes the finite size of the meson. The function  $\Phi_H$  must be invariant under the translation  $F_H(x + a, x_1 + a, x_2 + a) = F_H(x, x_1, x_2)$ .

In our previous papers we have used the so-called impulse approximation for the evaluation of the Feynman diagrams. In the impulse approximation one omits a possible dependence of the vertex functions on external momenta. The impulse approximation therefore entails a certain dependence on how loop momenta are routed through the diagram at hand. This problem no longer exists in the present full treatment where the impulse approximation is no longer used. In the present calculation we will use a particular form of the vertex function given by

$$F_H(x, x_1, x_2) = \delta\left(x - \frac{m_1 x_1 + m_2 x_2}{m_1 + m_2}\right) \Phi_H((x_1 - x_2)^2). \quad (55)$$

where  $m_1$  and  $m_2$  are the constituent quark masses. The vertex function  $F_H$  evidently satisfies the above translational invariance condition. As mentioned before we no longer use the impulse approximation in the present calculation.

The coupling constants  $g_H$  in Eq. (54) are determined by the so called *compositeness condition* proposed in [20] and extensively used in [21]. The compositeness condition means that the renormalization constant of the meson field is set equal to zero

$$Z_H = 1 - \frac{3g_H^2}{4\pi^2} \tilde{\Pi}'_H(m_H^2) = 0 \quad (56)$$

where  $\tilde{\Pi}'_H$  is the derivative of the meson mass operator. For the pseudoscalar and vector mesons treated in this paper one has

$$\begin{aligned} \tilde{\Pi}'_P(p^2) &= \frac{1}{2p^2} p^\alpha \frac{d}{dp^\alpha} \int \frac{d^4k}{4\pi^2 i} \tilde{\Phi}_P^2(-k^2) \\ &\quad \times \text{tr} \left[ \gamma^5 S_1(\not{k} + w_{21} \not{p}) \gamma^5 S_2(\not{k} - w_{12} \not{p}) \right] \\ \tilde{\Pi}'_V(p^2) &= \frac{1}{3} \left[ g^{\mu\nu} - \frac{p^\mu p^\nu}{p^2} \right] \frac{1}{2p^2} p^\alpha \frac{d}{dp^\alpha} \int \frac{d^4k}{4\pi^2 i} \tilde{\Phi}_V^2(-k^2) \\ &\quad \times \text{tr} \left[ \gamma^\nu S_1(\not{k} + w_{21} \not{p}) \gamma^\mu S_2(\not{k} - w_{12} \not{p}) \right] \end{aligned}$$

where  $w_{ij} = m_j/(m_i + m_j)$ ,  $\tilde{\Phi}_H(-k^2)$  is the Fourier-transform of the correlation function  $\Phi_H((x_1 - x_2)^2)$  and  $S_i(\not{k})$  is the quark propagator. The leptonic decay constant  $f_P$  is calculated from

$$\frac{3g_P}{4\pi^2} \int \frac{d^4k}{4\pi^2 i} \tilde{\Phi}_P(-k^2) \text{tr} \left[ O^\mu S_1(\not{k} + w_{21} \not{p}) \gamma^5 S_2(\not{k} - w_{12} \not{p}) \right] = f_P p^\mu. \quad (57)$$

The transition form factors  $P(p_1) \rightarrow P(p_2), V(p_2)$  can be calculated from the Feynman integral corresponding to the diagram of Fig. 2:

$$\begin{aligned} \Lambda^{\Gamma^\mu}(p_1, p_2) &= \frac{3g_P g_{P'(V)}}{4\pi^2} \int \frac{d^4k}{4\pi^2 i} \tilde{\Phi}_P(-(k + w_{13} p_1)^2) \tilde{\Phi}_{P'(V)}(-(k + w_{23} p_2)^2) \\ &\quad \times \text{tr} \left[ S_2(\not{k} + \not{p}_2) \Gamma^\mu S_1(\not{k} + \not{p}_1) \gamma^5 S_3(\not{k}) \Gamma_{\text{out}} \right] \end{aligned} \quad (58)$$

where  $\Gamma^\mu = \gamma^\mu$ ,  $\gamma^\mu \gamma^5$ ,  $i\sigma^{\mu\nu} q_\nu$ , or  $i\sigma^{\mu\nu} q_\nu \gamma^5$  and  $\Gamma_{P',V} = \gamma^5$ ,  $\gamma_\nu \epsilon_2^\nu$ .

We use the local quark propagators

$$S_i(\not{k}) = \frac{1}{m_i - \not{k}}, \quad (59)$$

where  $m_i$  is the constituent quark mass. We do not introduce a new notation for constituent quark masses in order to distinguish them from the current quark masses used in the effective Hamiltonian and Wilson coefficients as described in Sec. II because it should always be clear from the context which set of masses is being referred to. As discussed in [18, 19], we assume that

$$m_H < m_1 + m_2 \quad (60)$$

in order to avoid the appearance of imaginary parts in the physical amplitudes.

The fit values for the constituent quark masses are taken from our papers [18, 19] and are given in Eq. (61).

$$\begin{array}{ccccc} m_u & m_s & m_c & m_b & \text{GeV} \\ \hline 0.235 & 0.333 & 1.67 & 5.06 & \end{array} \quad (61)$$

It is readily seen that the constraint Eq. (60) holds true for the low-lying flavored pseudoscalar mesons but is no longer true for the vector mesons. In the case of the heavy mesons  $D^*$  and  $B^*$  we will employ identical masses for the vector mesons and the pseudoscalar mesons for the calculation of matrix elements in Eqs. (56), (57) and (58). It is a quite reliable approximation because of  $(m_{D^*} - m_D)/m_D \sim 7\%$  and  $(m_{B^*} - m_B)/m_B \sim 1\%$ .

We employ a Gaussian for the vertex function  $\tilde{\Phi}_H(k_E^2/\Lambda_H^2) = \exp(-k_E^2/\Lambda_H^2)$  where  $k_E$  is the Euclidean momentum and determine the size parameters  $\Lambda_H$  by a fit to the experimental data, when available, or to lattice simulations for the leptonic decay constants. The quality of the fit can be seen from Table 3. The branching ratios of the semileptonic decays are shown in Table 4. The numerical values for  $\Lambda_H$  are  $\Lambda_\pi = 1$  GeV,  $\Lambda_K = 1.6$  GeV,  $\Lambda_D = 2$  GeV and  $\Lambda_B = 2.25$  GeV for all  $K$ ,  $D$  and  $B$  partners, respectively.

We are now in a position to present our results for the  $B \rightarrow K$  form factors. We have used the technique outlined in our previous papers [18, 19] for the numerical evaluation of the Feynman integrals in Eq. (58). The results of our numerical calculations are well represented by the parametrization

$$F(s) = \frac{F(0)}{1 - as + bs^2}. \quad (62)$$

Using such a parametrization facilitates further integrations. The values of  $F(0)$ ,  $a$  and  $b$  are listed in Tables 5–6. We plot our form factors in Fig. 3 and compare them with those used in paper [8] in Fig. 4. The functional behavior of the curves is similar to each other.

At the end of this section we would like to discuss the impulse approximation used in our previous papers [18, 19]. It was simply assumed that the vertex functions depend only on the loop momentum flowing through the vertex. The explicit translational invariant vertex function in Eq. (55) allows one to check the reliability of this approximation. We found that the results obtained with and without the impulse approximation are rather close to each other except for the heavy-to-light form factors. We consider the  $B \rightarrow \pi$ -transition as an example to illustrate this point. The calculated values of the  $F_+^{B\pi}(q^2)$  form factor at  $q^2 = 0$  are

$$F_+^{B\pi}(0) = \begin{cases} 0.27 & \text{exact} \\ 0.48 & \text{impulse approximation} \end{cases}$$

One can see that the value of the form factor at  $q^2 = 0$  calculated without the impulse approximation is considerably smaller than when calculated with the

impulse approximation. Its value is close to the value of QCD SR estimates, see, for example, [29]:

$$F_+^{B\pi}(0) = \begin{cases} 0.25 & \text{asymptotic distribution} \\ 0.30 & \text{QCD SR distribution} \end{cases}$$

## 5 Numerical results

In this section we collect and discuss our numerical results. We plot the normalized differential distributions  $\Gamma_{\text{tot}}^{-1} d\Gamma/ds$  with  $\Gamma_{\text{tot}} = 1/\tau_B$  ( $\tau_B = (\tau_{B^0} + \tau_{B^+})/2 = 1.60 \text{ ps}$ ) and  $s = q^2/m_B^2$  in Figs. 5-6 for the decay  $B \rightarrow K\bar{l}l$ .

We have also included the  $B \rightarrow K\bar{\nu}\nu$  modes. Their differential rates are calculated according to

$$\frac{d\Gamma(B^+ \rightarrow K\bar{\nu}\nu)}{ds} = \frac{G_F^2 m_B^5 |\lambda_t|^2 \alpha^2 |D_\nu(x_t)|^2}{2^8 \pi^5 \sin^4 \theta_W} |F_+|^2 \phi_H^{\frac{3}{2}}. \quad (63)$$

The functions  $D_\nu(x_t)$  and  $\phi_H$  are given in Appendix B. The behavior of the normalized differential distributions is shown in Fig. 7.

We list our numerical results for the branching ratios in Table 7. When comparing the values of the branching ratios with those obtained in [8] one finds that they almost agree with each other.

Finally, we plot the dependence of the normalized differential distributions  $s = q^2/m_{B_c}^2$  in Figs. 10-12 for the decay  $B_c \rightarrow D(D^*)\bar{l}l(\bar{\nu}\nu)$ . In the numerical analysis we use the input parameters:  $m_{B_c} = 6.4 \text{ GeV}$ ,  $\tau_{B_c} = 0.46 \text{ ps}$  and  $|V_{td}^\dagger V_{tb}| = 0.008$ . The  $B_c \rightarrow D_d(D_d^*)$ -transition form factors are plotted in Figs. 8,9 and the normalized differential distributions for  $B_c \rightarrow D(D^*)\mu^+\mu^-$ ,  $B_c \rightarrow D(D^*)\tau^+\tau^-$  and  $B_c \rightarrow D(D^*)\bar{\nu}\nu$  are shown in Figs. 10,11,12, respectively. The results for the branching ratios are also given in Table 7. They are to be compared with the results of calculations performed in [17] where the light front and constituent quark models were employed.

## 6 Acknowledgments

This work was completed while M.A.I. visited the Universities of Mainz and Tübingen. M.A.I. appreciates the partial support by Plester Foundation, the DFG grants GRK683 and 436 RUS17/47/02, the Russian Fund of Basic Research grant No. 01-02-17200 and the Heisenberg-Landau Program. A.F., Th.G. and V.E.L. thank the DFG grants FA67/25-1 and GRK683 for support.

## References

1. R. Barate et al., ALEPH Coll.: Phys. Lett. B **429** (1998) 169.
2. K. Abe et al., Belle Coll.: Phys. Lett. B **511** (2001) 151.
3. S. Chen et al., CLEO Coll.: Phys. Rev. Lett. **87** (2001) 251807.
4. A. Ali, E. Lunghi, C. Greub, G. Hiller: Phys. Rev. D **66** (2002) 034002.
5. K. Abe et al., BELLE Coll.: Phys. Rev. Lett. **88** (2002) 021801.
6. F. Abe et al., CDF Coll.: Phys. Rev. Lett. **81** (1998) 2432; Phys. Rev. D **58** (1998) 112004.
7. G. Buchalla, A.J. Buras, M.E. Lautenbacher: Rev. Mod. Phys. **68** (1996) 1125; A.J. Buras, M. Munz: Phys. Rev. D **52** (1995) 186.
8. A. Ali, P. Ball, L.T. Handoko, G. Hiller: Phys. Rev. D **61** (2000) 074024.
9. C. Greub, A. Ioannissian, D. Wyler: Phys. Lett. B **346** (1995) 149.
10. P. Colangelo, F. De Fazio, P. Santorelli, E. Scrimieri: Phys. Rev. D **53** (1996) 3672 [Erratum-ibid. D **57** (1998) 3186].
11. D. Melikhov, N. Nikitin, S. Simula: Phys. Rev. D **57** (1998) 6814.
12. T.M. Aliev, M.K. Cakmak, A. Ozpineci, M. Savci: Phys. Rev. D **64** (2001) 055007; T.M. Aliev, M. Savci, A. Ozpineci, H. Koru: J. Phys. G **24** (1998) 49.
13. Q.S. Yan, C.S. Huang, W. Liao, S.H. Zhu: Phys. Rev. D **62** (2000) 094023.
14. F. Kruger, L.M. Sehgal, N. Sinha, R. Sinha: Phys. Rev. D **61** (2000) 114028 [Erratum-ibid. D **63** (2001) 019901].
15. F. Kruger, L.M. Sehgal: Phys. Lett. B **380** (1996) 199.
16. J.L. Hewett: Phys. Rev. D **53** (1996) 4964.
17. C.Q. Geng, C.W. Hwang, C.C. Liu: Phys. Rev. D **65** (2002) 094037.
18. M.A. Ivanov, M.P. Locher, V.E. Lyubovitskij: Few Body Syst. **21** (1996) 131; M.A. Ivanov, V.E. Lyubovitskij: Phys. Lett. B **408** (1997) 435; M.A. Ivanov, V.E. Lyubovitskij, J.G. Körner, P. Kroll: Phys. Rev. D **56** (1997) 348; M.A. Ivanov, J.G. Körner, V.E. Lyubovitskij, A.G. Rusetsky: Phys. Rev. D **57** (1998) 5632; D **60** (1999) 094002; Phys. Lett. B **476** (2000) 58; M.A. Ivanov, J.G. Körner, V.E. Lyubovitskij: Phys. Lett. B **448** (1999) 143; M.A. Ivanov, J.G. Körner, V.E. Lyubovitskij, M.A. Pisarev, A.G. Rusetsky: Phys. Rev. D **61** (2000) 114010.
19. M.A. Ivanov, P. Santorelli: Phys. Lett. B **456** (1999) 248; M.A. Ivanov, J.G. Körner, P. Santorelli: Phys. Rev. D **63** (2001) 074010; A. Faessler, T. Gutsche, M.A. Ivanov, J.G. Körner, V.E. Lyubovitskij: Phys. Lett. B **518** (2001) 55.
20. A. Salam: Nuovo Cim. **25** (1962) 224; S. Weinberg: Phys. Rev. **130** (1963) 776; K. Hayashi et al.: Fort. Phys. **15** (1967) 625.
21. G.V. Efimov, M.A. Ivanov: *The Quark Confinement Model Of Hadrons*. Bristol, UK: IOP 1993; Int. J. Mod. Phys. A **4** (1989) 2031.
22. M.A. Ivanov, Y.L. Kalinovsky, C.D. Roberts: Phys. Rev. D **60** (1999) 034018.
23. A. Ali, T. Mannel, T. Morozumi: Phys. Lett. B **273** (1991) 505.
24. J.G. Körner, G.A. Schuler: Z. Phys. C **38** (1988) 511 [Erratum-ibid. C **41** (1989) 690]; Z. Phys. C **46** (1990) 93.
25. C.S. Kim, Y.G. Kim, C.D. Lu, T. Morozumi: Phys. Rev. D **62** (2000) 034013.
26. A. Ali, A.S. Safir: arXiv:hep-ph/0205254.
27. C.H. Chen, C.Q. Geng: Nucl. Phys. B **636** (2002) 338. Phys. Rev. D **63** (2001) 114025.
28. D. Melikhov, N. Nikitin, S. Simula: Phys. Lett. B **442** (1998) 381.
29. E. Bagan, P. Ball, V.M. Braun: Phys. Lett. B **417** (1998) 154.
30. K. Hagiwara et al.: Phys. Rev. D **66** (2002) 010001.
31. S. Ryan: Nucl. Phys. B (Proc. Suppl.) **106** (2002) 86.
32. C.Q. Geng, C.P. Kao: Phys. Rev. D **57** (1998) 4479; D **54** (1996) 5636.

## Appendix A: Wilson Coefficients

In this paper we use the Wilson-coefficients  $C_i$  calculated in the naive dimensional regularization (NDR) scheme in the leading logarithmic approximation [7]:

$$\begin{aligned} C_j(\mu) &= \sum_{i=1}^8 k_{ji} \eta^{a_i} \quad (j = 1, \dots, 6) \\ C_7(\mu) &= \eta^{\frac{16}{23}} C_7(M_W) + \frac{8}{3} \left( \eta^{\frac{14}{23}} - \eta^{\frac{16}{23}} \right) C_8(M_W) + \sum_{i=1}^8 h_i \eta^{a_i}, \end{aligned}$$

with

$$\eta = \frac{\alpha(M_W)}{\alpha(\mu)}, \quad C_7(M_W) = -\frac{1}{2} A(x_t), \quad C_8(M_W) = -\frac{1}{2} F(x_t),$$

where  $x_t = m_t^2/M_W^2$  and  $A(x)$  and  $F(x)$  are defined below. The numbers  $a_i$ ,  $k_{ji}$  and  $h_i$  are given in Table 8.

The coefficient of  $Q_{10}$  is given by

$$C_{10}(M_W) = -\frac{Y(x_t)}{\sin^2 \Theta_W}$$

with  $Y(x)$  given below. Since  $Q_{10}$  is not subject to renormalization under QCD, its coefficient does not depend on  $\mu \approx \mathcal{O}(m_b)$ . The only renormalization scale dependence enters through the definition of the top quark mass.

Finally, including leading as well as next-to-leading logarithms, one finds

$$C_9(\mu) = P_0 + \frac{Y(x_t)}{\sin^2 \Theta_W} - 4Z(x_t) + P_E E(x_t)$$

with

$$\begin{aligned} P_0 &= \frac{\pi}{\alpha_s(M_W)} (-0.1875 + \sum_{i=1}^8 p_i \eta^{a_i+1}) + 1.2468 + \sum_{i=1}^8 \eta^{a_i} [r_i + s_i \eta] \\ P_E &= 0.1405 + \sum_{i=1}^8 q_i \eta^{a_i+1} \\ Y(x) &= C(x) - B(x), \quad Z(x) = C(x) + \frac{1}{4} D(x). \end{aligned}$$

Here

$$\begin{aligned} A(x) &= \frac{x(8x^2 + 5x - 7)}{12(x-1)^3} + \frac{x^2(2-3x)}{2(x-1)^4} \ln x, \\ B(x) &= \frac{x}{4(1-x)} + \frac{x}{4(x-1)^2} \ln x, \end{aligned}$$

$$\begin{aligned}
C(x) &= \frac{x(x-6)}{8(x-1)} + \frac{x(3x+2)}{8(x-1)^2} \ln x, \\
D(x) &= \frac{-19x^3 + 25x^2}{36(x-1)^3} + \frac{x^2(5x^2 - 2x - 6)}{18(x-1)^4} \ln x - \frac{4}{9} \ln x, \\
E(x) &= \frac{x(18 - 11x - x^2)}{12(1-x)^3} + \frac{x^2(15 - 16x + 4x^2)}{6(1-x)^4} \ln x - \frac{2}{3} \ln x, \\
F(x) &= \frac{x(x^2 - 5x - 2)}{4(x-1)^3} + \frac{3x^2}{2(x-1)^4} \ln x.
\end{aligned}$$

The coefficients  $p_i$ ,  $r_i$ ,  $s_i$ , and  $q_i$  are given in Table 8.

## Appendix B: The functions in Eqs. (31) and (63).

We list here a set of the functions appearing in Eqs. (31) and (63) from [8] and [17].

$$\begin{aligned}
\phi_H &= \left(1 - r_H\right)^2 - 2s\left(1 + r_H\right) + s^2, \\
D_\nu(x) &= \frac{x}{8} \left( \frac{2+x}{x-1} + \frac{3x-6}{(x-1)^2} \ln x \right) \\
\alpha_1 &= (1 - \sqrt{r_H})^2 \left| A_0 \right|^2 + \frac{\phi_H}{(1 + \sqrt{r_H})^2} \left| V \right|^2 \\
\beta_1 &= \frac{(1 - \sqrt{r_H})^2}{4r_H} \left| A_0 \right|^2 - \frac{s}{(1 + \sqrt{r_H})^2} \left| V \right|^2 + \frac{\phi_H \left| A_+ \right|^2}{4r_H(1 + \sqrt{r_H})^2} \\
&\quad - \frac{1}{2} \left( \frac{1-s}{r_H} - 1 \right) \frac{1 - \sqrt{r_H}}{1 + \sqrt{r_H}} \text{Re}(A_0 A_+^\dagger), \\
\alpha_2 &= \left| C_9^{\text{eff}} F_+ + \frac{2 \hat{m}_b C_7^{\text{eff}} F_T}{1 + \sqrt{r_H}} \right|^2 + |C_{10} F_+|^2, \\
\beta_2 &= |C_{10}|^2 \left[ \left( 1 + r_H - \frac{s}{2} \right) |F_+|^2 + \left( 1 - r_H \right) \text{Re}(F_+ F_-^\dagger) + \frac{1}{2} s |F_-|^2 \right], \\
\alpha_3 &= (1 - \sqrt{r_H})^2 \left[ \left| C_9^{\text{eff}} A_0 + \frac{2 \hat{m}_b C_7^{\text{eff}} (1 + \sqrt{r_H}) a_0}{s} \right|^2 + \left| C_{10} A_0 \right|^2 \right] \\
&\quad + \frac{\phi_H}{(1 + \sqrt{r_H})^2} \left[ \left| C_9^{\text{eff}} V + \frac{2 \hat{m}_b C_7^{\text{eff}} (1 + \sqrt{r_H}) g}{s} \right|^2 + \left| C_{10} V \right|^2 \right], \\
\beta_3 &= \frac{(1 - \sqrt{r_H})^2}{4r_H} \left[ \left| C_9^{\text{eff}} A_0 + \frac{2 \hat{m}_b C_7^{\text{eff}} (1 + \sqrt{r_H}) a_0}{s} \right|^2 + \left| C_{10} A_0 \right|^2 \right]
\end{aligned}$$

$$\begin{aligned}
& - \frac{s}{(1 + \sqrt{r_H})^2} \left[ \left| C_9^{\text{eff}} V + \frac{2\hat{m}_b C_7^{\text{eff}} (1 + \sqrt{r_H}) g}{s} \right|^2 + \left| C_{10} V \right|^2 \right] \\
& + \frac{\phi_H}{4r_H (1 + \sqrt{r_H})^2} \left[ \left| C_9^{\text{eff}} A_+ + \frac{2\hat{m}_b C_7^{\text{eff}} (1 + \sqrt{r_H}) a_+}{s} \right|^2 + \left| C_{10} A_+ \right|^2 \right] \\
& - \frac{1}{2} \left( \frac{1-s}{r_H} - 1 \right) \frac{1-\sqrt{r_H}}{1+\sqrt{r_H}} \text{Re} \left\{ \left[ C_9^{\text{eff}} A_0 + \frac{2\hat{m}_b C_7^{\text{eff}} (1 + \sqrt{r_H}) a_0}{s} \right] \right. \\
& \times \left. \left[ C_9^{\text{eff}} A_+ + \frac{2\hat{m}_b C_7^{\text{eff}} (1 + \sqrt{r_H}) a_+}{s} \right] + |C_{10}|^2 \text{Re}(A_0 A_+^\dagger) \right\}, \\
\delta & = \frac{|C_{10}|^2}{2(1 + \sqrt{r_H})^2} \left\{ -2\phi_H |V|^2 - 3(1 - r_H)^2 |A_0|^2 \right. \\
& + \frac{\phi_H}{4r_H} \left[ 2(1 + r_H) - s \right] |A_+|^2 \\
& \left. + \frac{\phi_H s}{4r_H} |A_-|^2 + \frac{\phi_H (1 - r_H)}{2r_H} \text{Re} \left( -A_0 A_+^\dagger - A_0 A_-^\dagger + A_+ A_-^\dagger \right) \right\},
\end{aligned}$$

where  $\hat{m}_b = m_b/m_B$ .

**Table 1.** Central values of the input parameters and the corresponding values of the Wilson coefficients used in the numerical calculations.

$m_W$	80.41 GeV	$C_1$	-0.248
$m_Z$	91.1867 GeV	$C_2$	1.107
$\sin^2 \theta_W$	0.2233	$C_3$	0.011
$m_c$	1.4 GeV	$C_4$	-0.026
$m_t$	173.8 GeV	$C_5$	0.007
$m_{b,\text{pole}}$	4.8 GeV	$C_6$	-0.031
$\mu$	$m_{b,\text{pole}}$	$C_7^{\text{eff}}$	-0.313
$\Lambda_{QCD}$	0.220 GeV	$C_9$	4.344
$\alpha^{-1}$	129	$C_{10}$	-4.669
$\alpha_s(m_Z)$	0.119	$C_0$	0.362
$ V_{ts}^\dagger V_{tb} $	0.0385		
$ V_{td}^\dagger V_{tb} $	0.008		
$ V_{ts}^\dagger V_{tb} / V_{cb} $	1		

**Table 2.** Bilinear combinations of the helicity amplitudes that enter in the four-fold decay distribution Eq. ( 37 ).

Definition	Property	Title
$H_U^{ij} = \text{Re} (H_+^i H_+^{\dagger j}) + \text{Re} (H_-^i H_-^{\dagger j})$	$H_U^{ij} = H_U^{ji}$	Unpolarized-transverse
$H_{IU}^{ij} = \text{Im} (H_+^i H_+^{\dagger j}) + \text{Im} (H_-^i H_-^{\dagger j})$	$H_{IU}^{ij} = -H_{IU}^{ji}$	
$H_P^{ij} = \text{Re} (H_+^i H_+^{\dagger j}) - \text{Re} (H_-^i H_-^{\dagger j})$	$H_P^{ij} = H_P^{ji}$	Parity-odd
$H_{IP}^{ij} = \text{Im} (H_+^i H_+^{\dagger j}) - \text{Im} (H_-^i H_-^{\dagger j})$	$H_{IP}^{ij} = -H_{IP}^{ji}$	
$H_T^{ij} = \text{Re} (H_+^i H_-^{\dagger j})$		Transverse-interference
$H_{IT}^{ij} = \text{Im} (H_+^i H_-^{\dagger j})$		
$H_L^{ij} = \text{Re} (H_0^i H_0^{\dagger j})$	$H_L^{ij} = H_L^{ji}$	Longitudinal
$H_{IL}^{ij} = \text{Im} (H_0^i H_0^{\dagger j})$	$H_{IL}^{ij} = -H_{IL}^{ji}$	
$H_S^{ij} = 3 \text{Re} (H_t^i H_t^{\dagger j})$	$H_S^{ij} = H_S^{ji}$	Scalar
$H_{IS}^{ij} = 3 \text{Im} (H_t^i H_t^{\dagger j})$	$H_{IS}^{ij} = -H_{IS}^{ji}$	
$H_{SL}^{ij} = \text{Re} (H_t^i H_0^{\dagger j})$		Scalar-Longitudinal-interference
$H_{ISL}^{ij} = \text{Im} (H_t^i H_0^{\dagger j})$		
$H_I^{ij} = \frac{1}{2} [\text{Re} (H_+^i H_0^{\dagger j}) + \text{Re} (H_-^i H_0^{\dagger j})]$		transverse-longitudinal-Interference
$H_{II}^{ij} = \frac{1}{2} [\text{Im} (H_+^i H_0^{\dagger j}) + \text{Im} (H_-^i H_0^{\dagger j})]$		
$H_A^{ij} = \frac{1}{2} [\text{Re} (H_+^i H_0^{\dagger j}) - \text{Re} (H_-^i H_0^{\dagger j})]$		parity-Asymmetric
$H_{IA}^{ij} = \frac{1}{2} [\text{Im} (H_+^i H_0^{\dagger j}) - \text{Im} (H_-^i H_0^{\dagger j})]$		
$H_{ST}^{ij} = \frac{1}{2} [\text{Re} (H_+^i H_t^{\dagger j}) + \text{Re} (H_-^i H_t^{\dagger j})]$		Scalar-Transverse-interference
$H_{IST}^{ij} = \frac{1}{2} [\text{Im} (H_+^i H_t^{\dagger j}) + \text{Im} (H_-^i H_t^{\dagger j})]$		
$H_{SA}^{ij} = \frac{1}{2} [\text{Re} (H_+^i H_t^{\dagger j}) - \text{Re} (H_-^i H_t^{\dagger j})]$		Scalar-Asymmetric-interference
$H_{ISA}^{ij} = \frac{1}{2} [\text{Im} (H_+^i H_t^{\dagger j}) - \text{Im} (H_-^i H_t^{\dagger j})]$		

**Table 3.** Leptonic decay constants  $f_H$  (MeV) used in the least-square fit. The values are taken either from PDG [30] or from the Lattice [31]: quenched (upper line) and unquenched (lower line).

Meson	This model	Expt/Lattice
$\pi^+$	131	$130.7 \pm 0.1 \pm 0.36$
$K^+$	161	$159.8 \pm 1.4 \pm 0.44$
$D^+$	211	$203 \pm 14$ $226 \pm 15$
$D_s^+$	222	$230 \pm 14$ $250 \pm 30$
$B^+$	180	$173 \pm 23$ $198 \pm 30$
$B_s^0$	196	$200 \pm 20$ $230 \pm 30$
$B_c^+$	398	

**Table 4.** Semileptonic decay branching ratios.

Meson	This model	Expt.
$\pi^+ \rightarrow \pi^0 l^+ \nu$	$1.03 \cdot 10^{-8}$	$(1.025 \pm 0.034) \cdot 10^{-8}$
$K^+ \rightarrow \pi^0 l^+ \nu$	$4.62 \cdot 10^{-2}$	$(4.82 \pm 0.06) \cdot 10^{-2}$
$B^+ \rightarrow D^0 l^+ \nu$	$2.40 \cdot 10^{-2}$	$(2.15 \pm 0.22) \cdot 10^{-2}$
$B^+ \rightarrow D^{*0} l^+ \nu$	$5.60 \cdot 10^{-2}$	$(5.3 \pm 0.8) \cdot 10^{-2}$
$B_c^+ \rightarrow D^0 l^+ \nu$	$2.05 \cdot 10^{-5}$	
$B_c^+ \rightarrow D^{*0} l^+ \nu$	$3.60 \cdot 10^{-5}$	

**Table 5.** Parameter values for the approximated form factors  $F(s) = F(0)/(1 - as + bs^2)$  ( $s = q^2/m_B^2$ ) in the decays  $B \rightarrow K\bar{l}l$ .

	$F_+$	$F_-$	$F_T$
$F(0)$	0.357	-0.275	0.337
$a$	1.011	1.050	1.031
$b$	0.042	0.067	0.051

**Table 6.** Parameter values for the approximated form factors  $F(s) = F(0)/(1 - as + bs^2)$  ( $s = q^2/m_B^2$ ) in the decays  $B_c \rightarrow D(D^*)\bar{l}l$ .

	$F_+$	$F_-$	$F_T$	$A_0$	$A_+$	$A_-$	$V$	$a_0$	$a_+$	$g$
$F(0)$	0.186	-0.190	0.275	0.279	0.156	-0.321	0.290	0.178	0.178	0.179
$a$	2.48	2.44	2.40	1.30	2.16	2.41	2.40	1.21	2.14	2.51
$b$	1.62	1.54	1.49	0.149	1.15	1.51	1.49	0.125	1.14	1.67

**Table 7.** Decay branching ratios without (with) long distance contributions.

Ref.	$\text{Br}(B \rightarrow K \mu^+ \mu^-)$	$\text{Br}(B \rightarrow K \tau^+ \tau^-)$	$\text{Br}(B \rightarrow K \bar{\nu}\nu)$
[8]	$0.57 \cdot 10^{-6}$	$1.3 \cdot 10^{-7}$	
[4]	$(0.35 \pm 0.12) \cdot 10^{-6}$		
[11]	$0.44 \cdot 10^{-6}$	$1.0 \cdot 10^{-7}$	$5.6 \cdot 10^{-6}$
[32]	$0.5 \cdot 10^{-6}$	$1.3 \cdot 10^{-7}$	
our	$0.55 (0.51) \cdot 10^{-6}$	$1.01 (0.87) \cdot 10^{-7}$	$4.19 \cdot 10^{-6}$

	our	[17]
$\text{Br}(B_c \rightarrow D_d \mu^+ \mu^-)$	$0.44 (0.38) \cdot 10^{-8}$	$0.41 (0.33) \cdot 10^{-8}$
$\text{Br}(B_c \rightarrow D_d^* \mu^+ \mu^-)$	$0.71 (0.58) \cdot 10^{-8}$	$1.01 (0.78) \cdot 10^{-8}$
$\text{Br}(B_c \rightarrow D_s \mu^+ \mu^-)$	$0.97 (0.86) \cdot 10^{-7}$	$1.36 (1.12) \cdot 10^{-7}$
$\text{Br}(B_c \rightarrow D_s^* \mu^+ \mu^-)$	$1.76 (1.41) \cdot 10^{-7}$	$4.09 (3.14) \cdot 10^{-7}$
$\text{Br}(B_c \rightarrow D_d \tau^+ \tau^-)$	$0.11 (0.09) \cdot 10^{-8}$	$0.13 (0.11) \cdot 10^{-8}$
$\text{Br}(B_c \rightarrow D_d^* \tau^+ \tau^-)$	$0.11 (0.08) \cdot 10^{-8}$	$0.18 (0.13) \cdot 10^{-8}$
$\text{Br}(B_c \rightarrow D_s \tau^+ \tau^-)$	$0.22 (0.18) \cdot 10^{-7}$	$0.34 (0.27) \cdot 10^{-7}$
$\text{Br}(B_c \rightarrow D_s^* \tau^+ \tau^-)$	$0.22 (0.15) \cdot 10^{-7}$	$0.51 (0.34) \cdot 10^{-7}$
$\text{Br}(B_c \rightarrow D_d \bar{\nu}\nu)$	$3.28 \cdot 10^{-8}$	
$\text{Br}(B_c \rightarrow D_d^* \bar{\nu}\nu)$	$5.78 \cdot 10^{-8}$	
$\text{Br}(B_c \rightarrow D_s \bar{\nu}\nu)$	$0.73 \cdot 10^{-6}$	
$\text{Br}(B_c \rightarrow D_s^* \bar{\nu}\nu)$	$1.42 \cdot 10^{-6}$	

**Table 8.** Values of parameters in the formulae for the Wilson coefficients.

$i$	1	2	3	4	5	6	7	8
$a_i$	$\frac{14}{23}$	$\frac{16}{23}$	$\frac{6}{23}$	$-\frac{12}{23}$	0.4086	-0.4230	-0.8994	0.1456
$k_{1i}$	0	0	$\frac{1}{2}$	$-\frac{1}{2}$	0	0	0	0
$k_{2i}$	0	0	$\frac{1}{2}$	$\frac{1}{2}$	0	0	0	0
$k_{3i}$	0	0	$-\frac{1}{14}$	$\frac{1}{6}$	0.0510	-0.1403	-0.0113	0.0054
$k_{4i}$	0	0	$-\frac{1}{14}$	$-\frac{1}{6}$	0.0984	0.1214	0.0156	0.0026
$k_{5i}$	0	0	0	0	-0.0397	0.0117	-0.0025	0.0304
$k_{6i}$	0	0	0	0	0.0335	0.0239	-0.0462	-0.0112
$h_i$	2.2996	-1.0880	$-\frac{3}{7}$	$-\frac{1}{14}$	-0.6494	-0.0380	-0.0185	-0.0057
$\bar{h}_i$	0.8623	0	0	0	-0.9135	0.0873	-0.0571	0.0209
$p_i$	0	0	$-\frac{80}{203}$	$\frac{8}{33}$	0.0433	0.1384	0.1648	-0.0073
$r_i$	0	0	0.8966	-0.1960	-0.2011	0.1328	-0.0292	-0.1858
$s_i$	0	0	-0.2009	-0.3579	0.0490	-0.3616	-0.3554	0.0072
$q_i$	0	0	0	0	0.0318	0.0918	-0.2700	0.0059

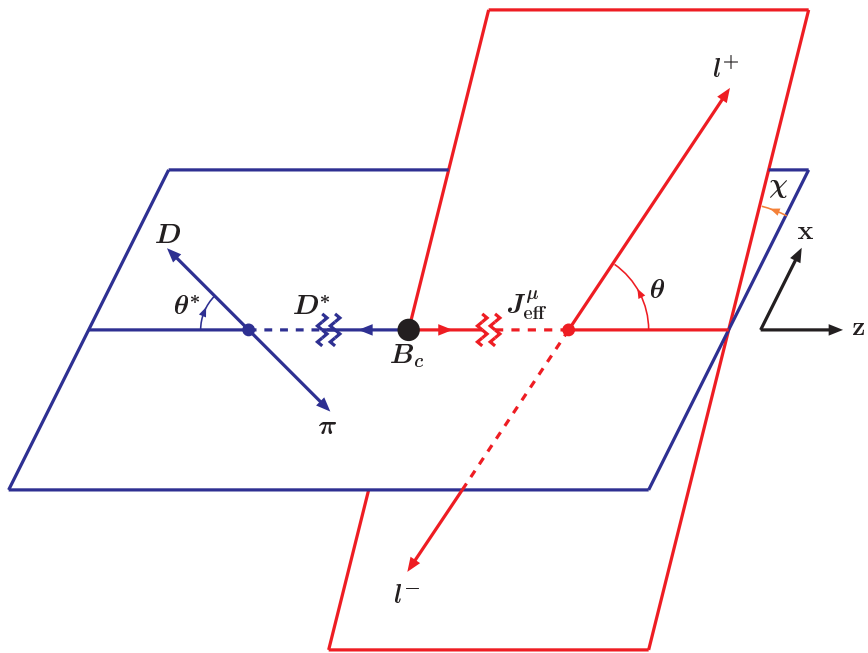


**Fig. 1.** Definition of angles  $\theta$ ,  $\theta^*$  and  $\chi$  in the cascade decay  $B_c \rightarrow D^* (\rightarrow D\pi) l\bar{l}$ .

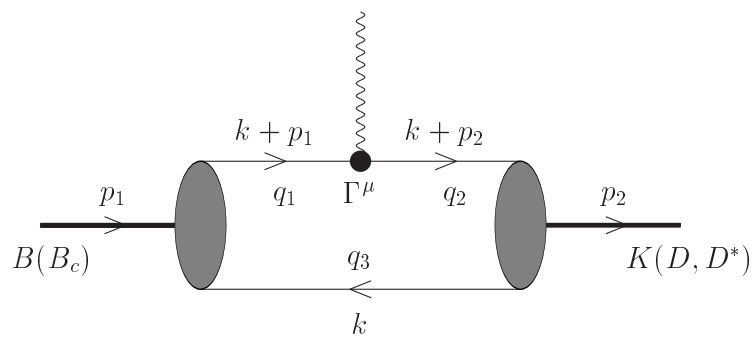


**Fig. 2.** Diagram describing the form factors of the decay  $B(B_c) \rightarrow K(D, D^*) l\bar{l}$

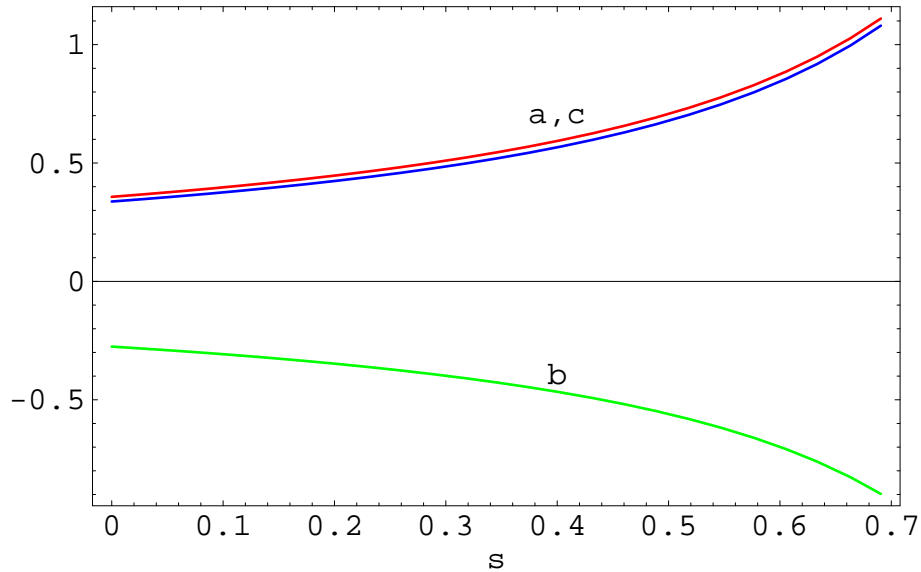


**Fig. 3.** Form factors for the  $B \rightarrow K$  transition: (a)  $F_+$ , (b)  $F_-$ , (c)  $F_T$ .

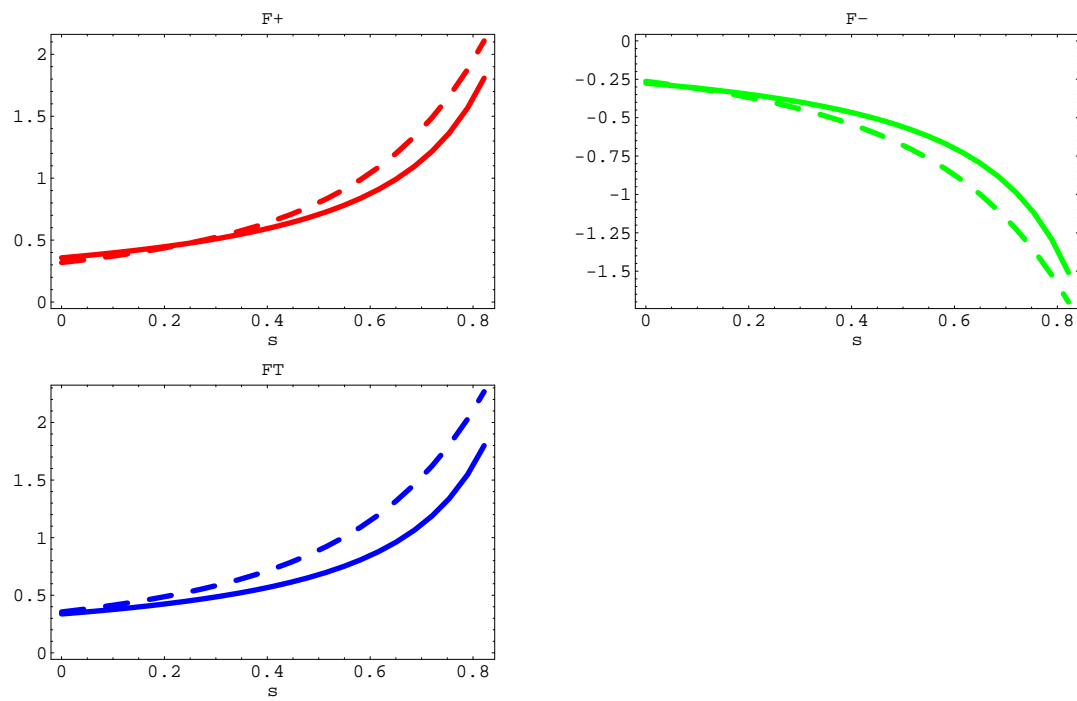


**Fig. 4.** Comparison of our  $B \rightarrow K$  form factors (solid line) with those used in [8] (dashed line).

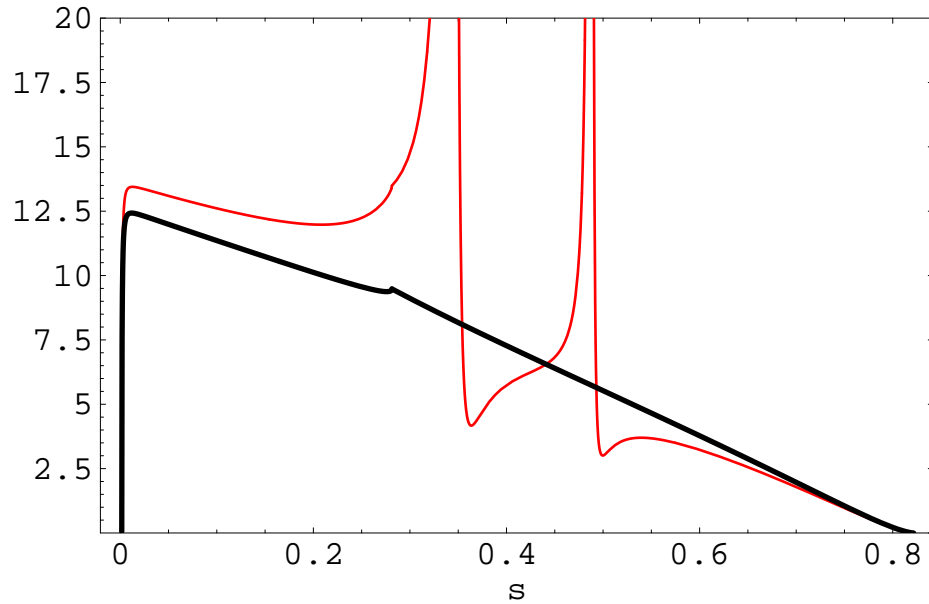


**Fig. 5.** Normalized differential distributions  $10^7 \Gamma_{\text{tot}}^{-1} d\Gamma/ds$  for  $B \rightarrow K \mu^+ \mu^-$ . The curves with resonant shapes represent long-distance contributions.

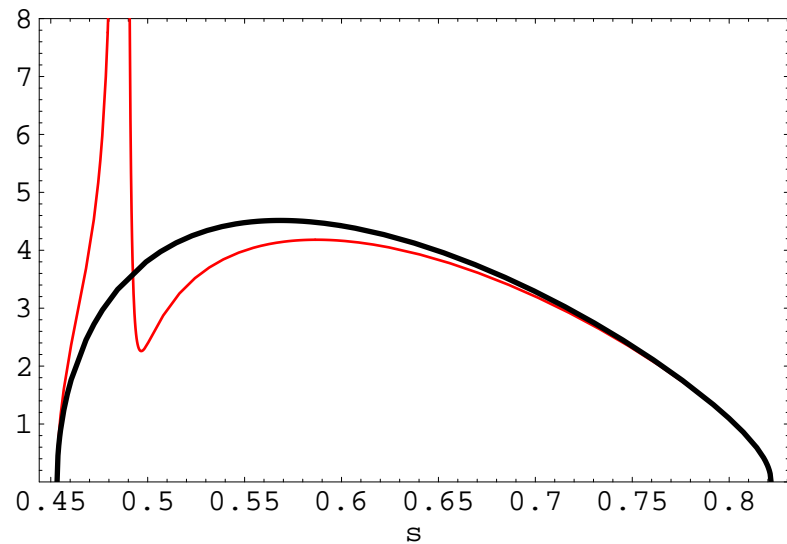


**Fig. 6.** Normalized differential distributions  $10^7 \Gamma_{\text{tot}}^{-1} d\Gamma/ds$  for  $B \rightarrow K \tau^+ \tau^-$ .

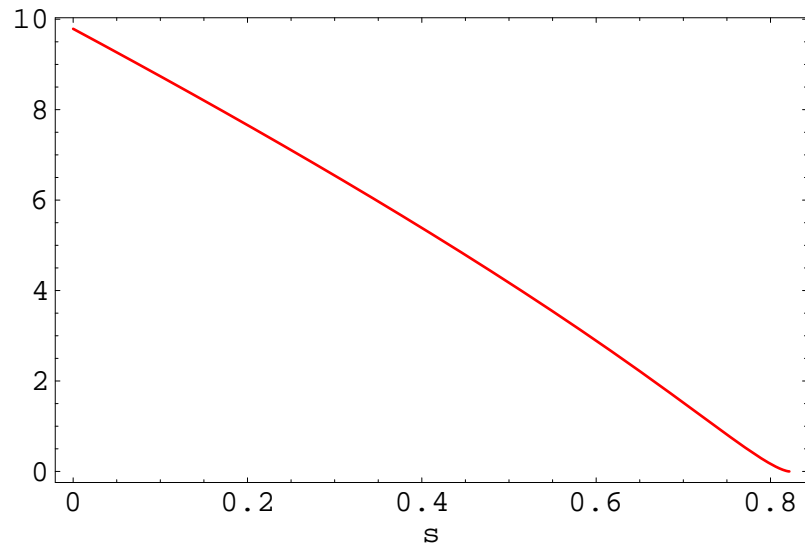


**Fig. 7.** Normalized differential distributions  $10^8 \Gamma_{\text{tot}}^{-1} d\Gamma/ds$  for  $B \rightarrow K \bar{\nu}\nu$ .

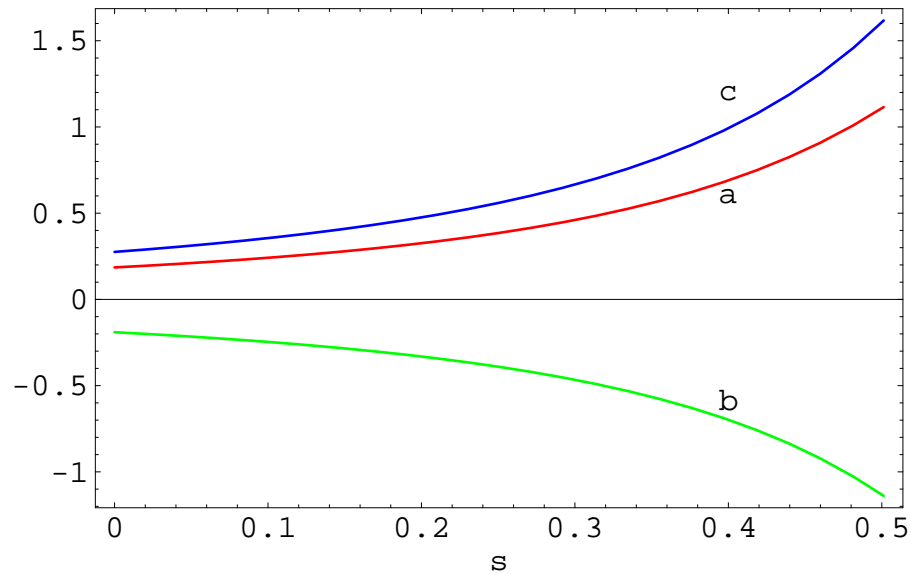


**Fig. 8.** Form factors for the  $B_c \rightarrow D_d$  transition: (a)  $F_+$ , (b)  $F_-$ , (c)  $F_T$ .

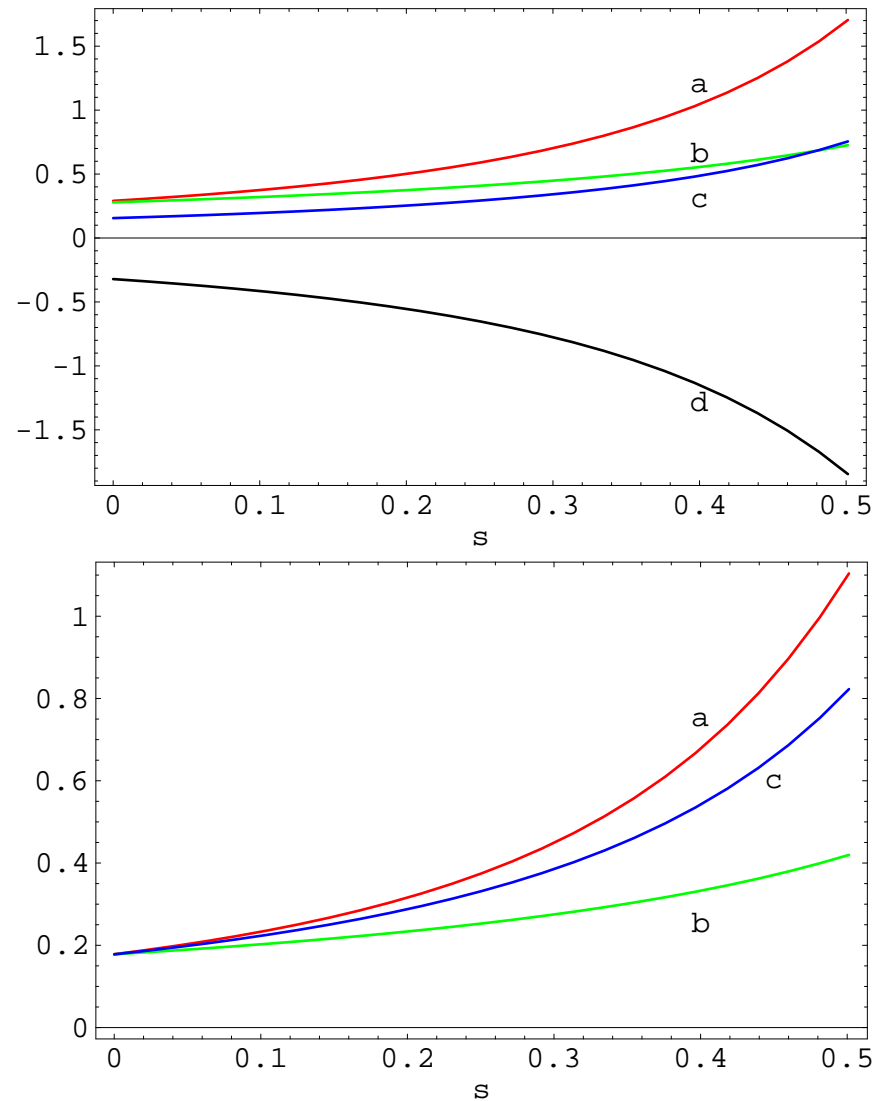


**Fig. 9.** Form factors for the  $B_c \rightarrow D_d^*$  transition. Upper panel: (a)  $V$ , (b)  $A_0$ , (c)  $A_+$ , (d)  $A_-$ . Lower panel: (a)  $g$ , (b)  $a_0$ , (c)  $a_+$ .

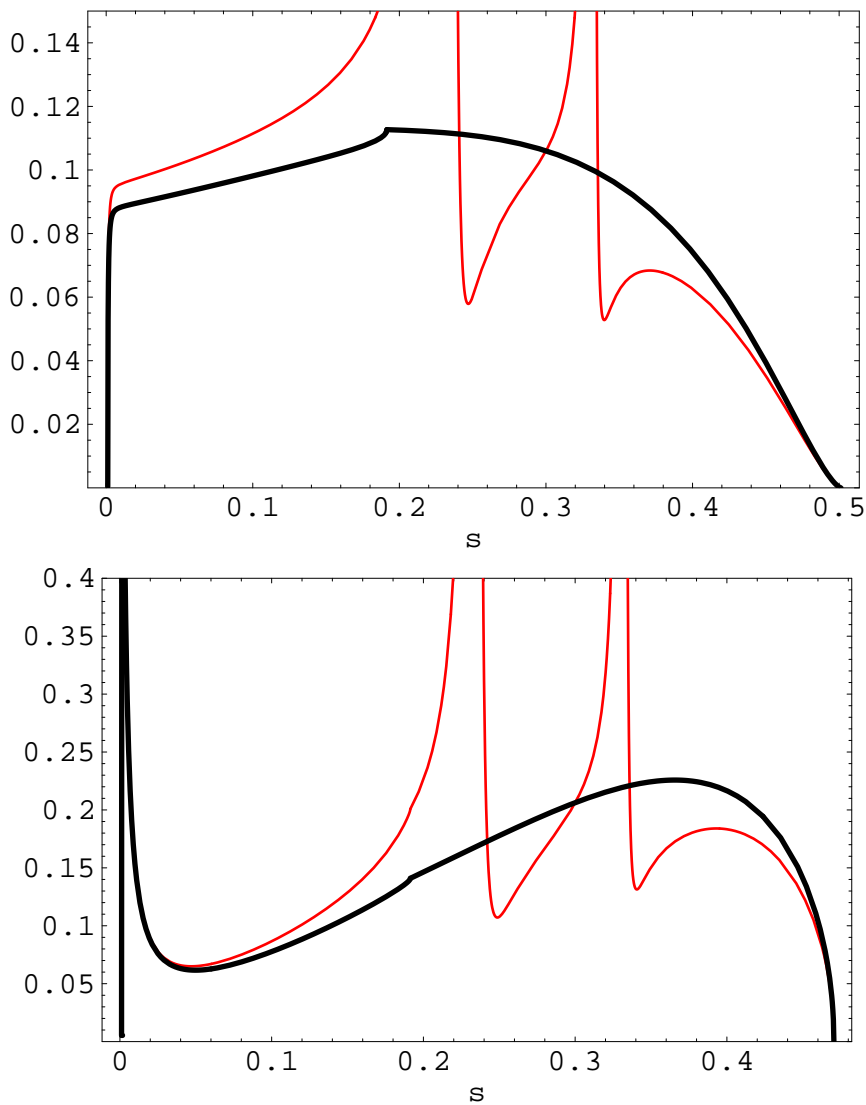


**Fig. 10.** Normalized differential distributions  $10^7 \Gamma_{\text{tot}}^{-1} d\Gamma/ds$  for  $B_c \rightarrow D \mu^+ \mu^-$  (upper panel) and  $B_c \rightarrow D^* \mu^+ \mu^-$  (lower panel).

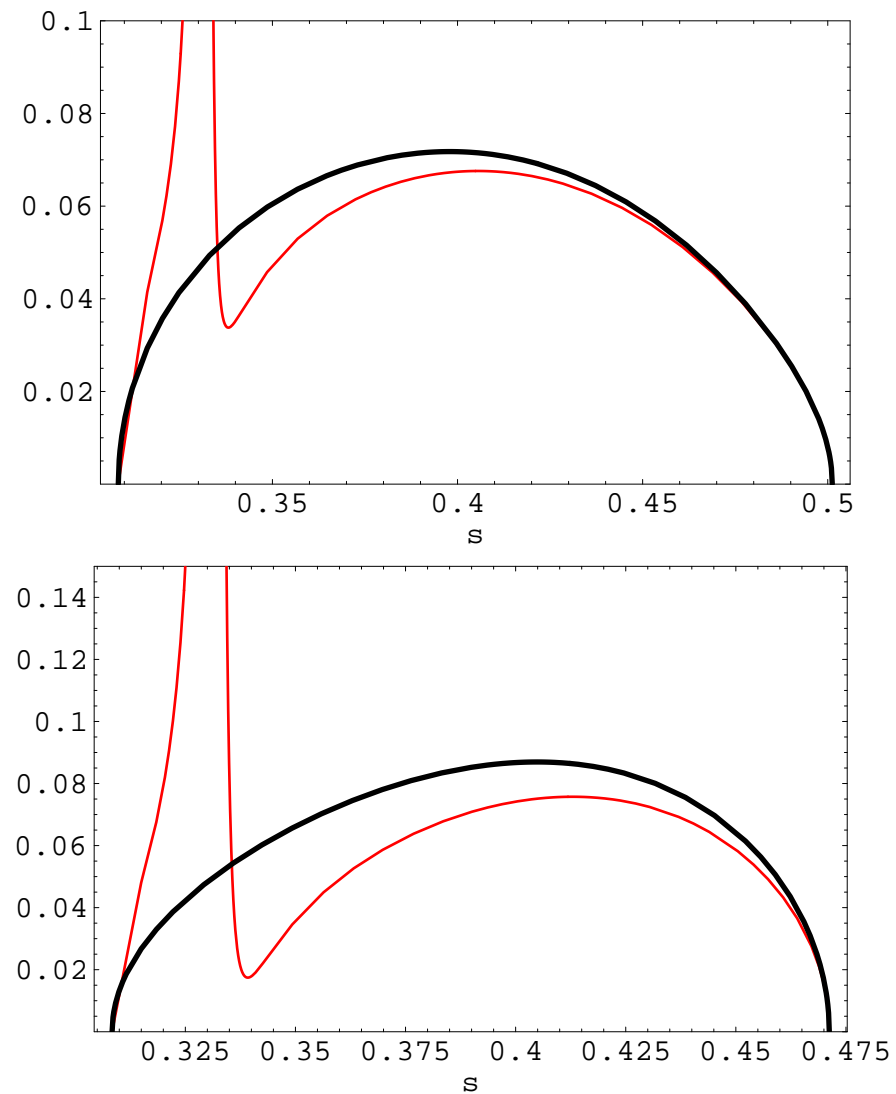


**Fig. 11.** Normalized differential distributions  $10^7 \Gamma_{\text{tot}}^{-1} d\Gamma/ds$  for  $B_c \rightarrow D \tau^+ \tau^-$  (upper panel) and  $B_c \rightarrow D^* \tau^+ \tau^-$  (lower panel).

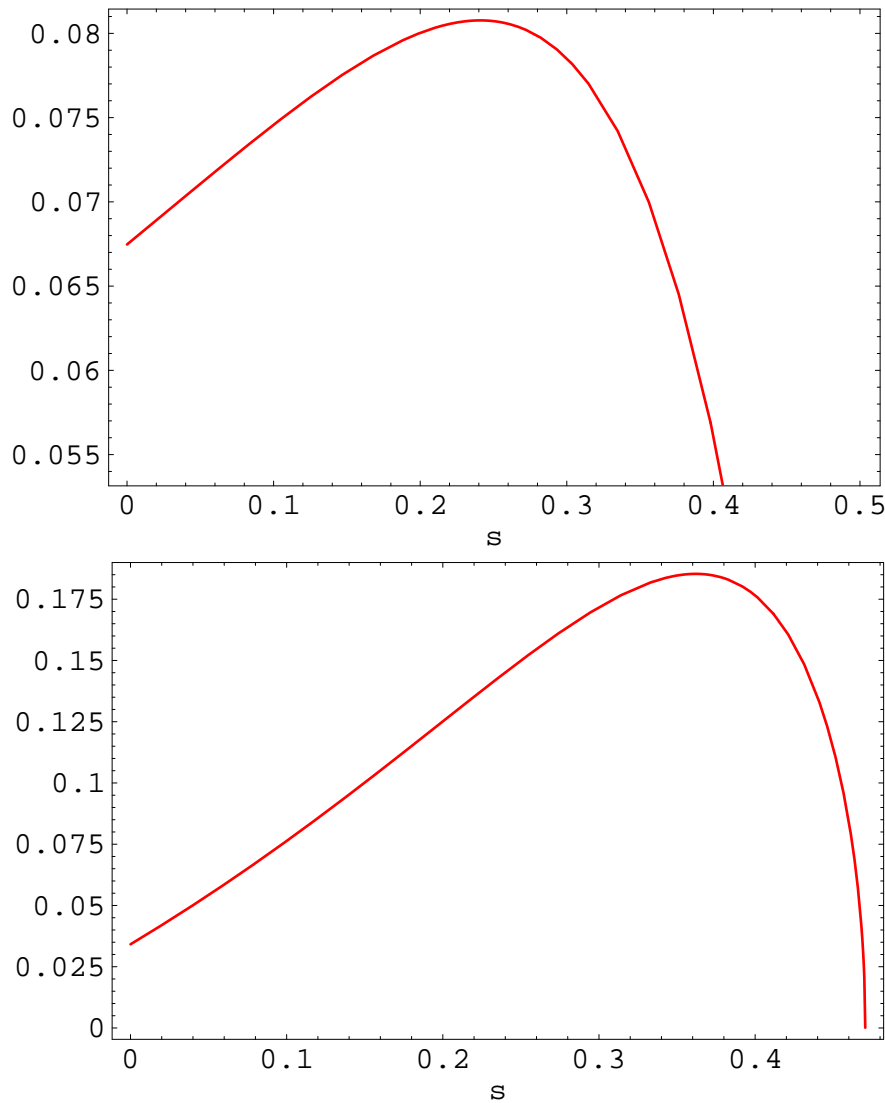


**Fig. 12.** Normalized differential distributions  $10^7 \Gamma_{\text{tot}}^{-1} d\Gamma/ds$  for  $B_c \rightarrow D \bar{\nu}\nu$  (upper panel) and  $B_c \rightarrow D^* \bar{\nu}\nu$  (lower panel).